



# Conceptual Design and Process Simulation of Methanol Synthesis from Glycerol

Bahizire Martin Mukeru<sup>1</sup> · Bilal Patel<sup>1</sup>

Received: 25 March 2022 / Revised: 29 July 2022 / Accepted: 1 August 2022 / Published online: 17 August 2022  
© The Author(s), under exclusive licence to Springer Nature Singapore Pte Ltd. 2022

## Abstract

Glycerol is considered as the main by-product during the production of biodiesel. Using glycerol as a biorefinery feedstock cannot only promote a circular biodiesel production but also alleviate waste management challenges. An insight-based approach (CHO ternary diagrams) was used in this study for the synthesis of methanol from glycerol via reforming processes. It was shown that to produce syngas that fulfils the requirement for methanol synthesis, glycerol should be co-fed with methane in a molar ratio of 1:2 using steam as a reforming agent. A high-level economic as well as environmental analysis was conducted. It was found that the price of glycerol has a significant impact on the economic potential of the process. The glycerol price at which the economic potential was zero was found to be approximately \$ 0.93/kg. It was shown that the process has a maximum carbon efficiency and atom economy with no waste generation (100% carbon efficiency and atom economy and 0 E-factor). Based on these CHO ternary diagram targets, a process simulation for methanol synthesis was developed using Aspen Plus. It was further revealed that Aspen Plus does not exceed targets set by CHO ternary diagrams (in terms of methanol production rate, carbon efficiency and atom economy).

**Keywords** CHO ternary diagrams · Glycerol biorefinery · Carbon deposition boundary · Aspen plus · Methanol synthesis · Process synthesis

## Nomenclature

CHO	Carbon-hydrogen-oxygen
%C	Carbon efficiency
E-factor	Environmental factor
EP	Economic potential (US \$)
GSR	Glycerol steam reforming
GPO	Glycerol partial oxidation
GDR	Glycerol dry reforming
$\Delta G^0$	Change in Gibbs energy at 298 K (kJ/mol)
$\Delta G_f^0$	Change in Gibbs energy of formation at 298 K (kJ/mol)
$\frac{H}{O}$	Hydrogen to oxygen ratio
IR	Independent reaction
$K_e$	Equilibrium constant
$M_i$	Molecular weight of component $i$ (kg/mol)
$n_i$	Stoichiometric coefficient of component $i$ (mol)

SGR	Steam to glycerol ratio
$x_i$	Mole composition of component $i$

## Introduction

Amongst the different types of renewable resources, biomass is the only resource that contains renewable carbon. This characteristic makes biomass a unique alternative source of energy and chemicals. A biorefinery is defined as the processing of raw materials (biomass) into chemicals and fuels with high economic value (IEA, 2012b). There are numerous types of biomass that are available for a biorefinery. Some of these types include energy and food crops, algae, industrial, forestry and agricultural residues and municipal solid waste (Tursi 2019).

The effective utilization of biomass as a biorefinery feedstock for the generation of transportation biofuels (such as biodiesel, methanol and ethanol) and other related biofuels (such as hydrogen and dimethyl ether) as well as high value chemicals has gained interest in recent years. Producing these biofuels and other commodities from biomass not only assists in combating climate change and reducing the global

✉ Bilal Patel  
patelb@unisa.ac.za

Bahizire Martin Mukeru  
martinmukeru@gmail.com

<sup>1</sup> Department of Chemical Engineering, University of South Africa, Florida, Roodepoort 1709, South Africa

reliance on petroleum but could also play a significant role in developing rural areas, creating job opportunities and investment in these areas (Pradhan and Mbohwa 2014).

Biofuel (bioethanol and biodiesel) production has significantly increased worldwide in recent years, from 128 (73.3 % bioethanol and 26.7 % biodiesel) to 140.2 (66.9% bioethanol and 33.1% biodiesel) billion litres in 2016 and 2018 respectively (WBA 2020). While in 2019, the production of biofuel worldwide reached approximately 161 billion litres (71.4 % bioethanol and 28.6 % biodiesel). This increase was curtailed in 2020 due to the COVID-19 pandemic. This pandemic caused the global biofuel production to decrease to 152 billion litres in 2020 (69.1 % bioethanol and 30.9 % biodiesel). The USA and Brazil were the leading biofuel producers in 2020 with 36 and 26% respectively (REN21 2021). The global production of biofuel is forecasted to increase and reach approximately 182 billion litres (72.5 % bioethanol and 27.5 % biodiesel) in 2030 (OEDC/FAO 2021). This continued growth of biofuel production is due to the fact that various countries have adopted biofuel policies and targets (Pradhan and Mbohwa 2014). For example, the European Union Directive (2009/28/EC) and 2018/2001 stipulated that all country members were required to use 10 % and 14 % of biofuel in transportation sector at the end of 2020 and 2030 respectively (EU 2009) and (EU 2018).

Many researchers have considered biodiesel as one of the most promising biofuels. Biodiesel generation is seen as a promising alternative to produce clean, biodegradable, non-toxic and renewable fuels (Harabi et al. 2019). This biofuel can also serve as an additive for conventional diesel (Asri 2018). It can be utilized alone without mixing it with any other fuel (Murillo et al. 2007), or as a mixture with diesel, for example B5 (where 5% of biodiesel is mixed with 95% diesel) (Kousoulidou et al. 2010). Animal tallow, vegetable or waste cooking oils serve as feedstock to produce biodiesel via a process called transesterification. A homogeneous or heterogeneous catalyst is typically required.

However, various wastes are generated such as glycerol, unconverted methanol/ethanol, biodiesel washing wastewaters and solid residues (Plácido and Capareda 2016). During the production of biodiesel, 10 to 20% by volume of glycerol is generated, and therefore, it is considered as the main by-product of biodiesel. In other words, if 100 L of biodiesel are to be produced, at least 10 L of crude glycerol is obtained. This means that a high production of biodiesel will always lead to considerable quantities of glycerol (D'Avino et al. 2015). For example, biodiesel industries approximately generated 3.42 billion litres of crude glycerol in 2016 and this production increased to 3.6 billion litres in 2018. It is estimated that this trend will keep on increasing and reach approximately 5 billion litres in 2030 (WBA 2020).

An increase in biodiesel global production has not only caused a dramatic reduction in crude glycerol pricing in recent years but also has raised environmental concerns due to the

way glycerol is disposed, because crude glycerol is a contaminated by-product. The price of crude glycerol has dropped significantly in recent years from \$3200/ton to \$500/ton in European Union and from \$2000/ton to \$600/ton in the USA due to a fast growth of biodiesel production (Bagnato et al. 2017). Despite these low prices of crude glycerol, the cost involved in its purification is exceedingly high and therefore this limits its applications as a purified product (Harabi et al. 2019).

Presently, some industries are utilizing glycerol as an additive to produce various products. Soap and cosmetics industries consume 28% of glycerol whereas other industries like polyglycerol, food and beverage industries consume more than 47% of glycerol. However, these applications will not accommodate an oversupply of crude glycerol. This means that the demand of crude glycerol will be less than its supply (Seadira et al. 2018).

It is crucial to look for alternative industrial uses of crude glycerol to improve and promote the biodiesel industry's economic viability. The economy of biodiesel depends on the way crude glycerol is utilized by various industries (Fan et al. 2010). The sustainable utilization of crude glycerol as a biorefinery feedstock to produce various products with high economic value will not only promote biodiesel production, but also contribute to its economy and ease pressure on waste management. Glycerol-based biorefineries are able to produce more than two thousand products via different industrial processes such as biochemical and thermochemical (Rodrigues et al. 2017).

It is possible to valorize crude glycerol via thermochemical routes such as reforming, pyrolysis and combustion (Kaur et al. 2020). Glycerol can undergo several reforming processes such as steam reforming (GSR), partial oxidation (GPO) and dry reforming (GDR) to produce syngas (a mixture of  $H_2$  and  $CO$ ) (Freitas and Guirardello 2014). Kale and Kulkarni (2010) conducted a thermodynamic analysis of glycerol reforming using a combination of  $CO_2$  and  $O_2$  as reforming agents in a temperature range of 327–727 °C and at a pressure of 1 bar. It was shown that a combination of dry reforming with partial oxidation of glycerol should be operated at a temperature of 653.13 °C, an oxygen to carbon (from glycerol) ratio of 0.3, a carbon dioxide to glycerol ratio of 1 and a pressure of 1 bar. This is due to the fact that these operating conditions produced a high yield of syngas (4.8 mol per mol of glycerol) with less methane and solid carbon.

Adhikari et al. (2007) applied the minimization of Gibbs energy to model the transformation of glycerol into  $H_2$  and  $CO$  by using  $H_2O$  as a reforming agent. It was revealed that increasing the temperature and SGR produced a high yield of  $H_2$  while the production of  $CO$  is minimized. For example, at a temperature, pressure and SGR (steam to glycerol ratio) of 1000 K, 1 atm and 9:1 respectively, roughly 6 moles of  $H_2$  were produced. While at the same conditions, roughly 1 mole of  $CO$  was generated. Wan (2010)

used the minimization of Gibbs energy to study the thermodynamic analysis of glycerol partial oxidation (using  $O_2$  as a reforming agent) for the synthesis of hydrogen. The optimal conditions for hydrogen synthesis such as reaction temperatures (727–827 °C) and oxygen to glycerol ratios (OGRs) (0.4–0.6) were identified. At these conditions, glycerol was completely converted while the yield  $H_2$  was 78.93% at an OGR of 0.4 and 87.31% at a ratio of 0.6. Freitas and Guirardello (2014) studied glycerol dry reforming (using  $CO_2$  as a reforming agent) process using the minimization of Gibbs energy at different temperatures, constant  $CO_2/C_3H_8O_3$  ratio (3:1) and at a pressure of 1 bar. It was revealed that higher composition of CO than  $H_2$  was generated at temperatures above 973 K and the syngas ratio was close to 1. For example, a temperature of 800 K produced a syngas ratio of 1.17 (29%  $H_2$  and 24.7% CO). While at 973 K, 43.7% and 32.1 % of CO and  $H_2$  was generated respectively. Even though the above cited works provide important guidelines in determining the optimal conditions for glycerol reforming, these works only focused on producing syngas from glycerol. Dang et al. (2022) studied the effect of certain impurities (methanol, acetic acid and oleic acid) during the glycerol steam reforming for hydrogen production. It was observed that at a fixed temperature, an impure glycerol (85% glycerol and 15% methanol) generated a higher hydrogen yield than pure glycerol, 97% glycerol-3% acetic acid and 98% glycerol-2% oleic acid. It was further observed that the yield of CO changes only slightly with glycerol purity. Thus, considering pure glycerol would produce a conservative estimate of the syngas yield.

There are only few studies on utilizing the glycerol-derived syngas in downstream processes such as methanol and FT-fuel synthesis. Gutiérrez Ortiz et al. (2013), Hunpinyo and Narataruksa (2016) and Mahabir et al. (2021) have shown that it is possible to utilize glycerol-derived syngas for the synthesis of methanol, hydrogen and FT-fuels using Aspen Plus. Mahabir et al. (2021) synthesized methanol through glycerol autothermal reforming and it was shown that this methanol can still be used in biodiesel industries. Gutiérrez Ortiz et al. (2013) synthesized methanol from glycerol-derived syngas via supercritical water reforming. Using this process, 0.27 kg of methanol per kilogram of glycerol was obtained. Hunpinyo and Narataruksa (2016) used Aspen Plus to design a process for the synthesis of hydrogen and FT-liquid fuels from glycerol reforming using steam as a reforming agent. It was shown that using 160 kmol/day of glycerol can produce a hydrogen yield of 75%. It was further shown that the same feed was used to generate 2692 L FT-liquid fuels ( $C_5$ - $C_{20}$ ) per day. This corresponds to a carbon efficiency of 31.38% (considering a hydrocarbon with 20 carbon atoms). Even though these works have extended the usefulness of glycerol reforming into the synthesis of specific products, it is important to determine the

performance of such processes prior to a detailed design. For example, one can quickly determine whether a specific alternative will produce waste and such an alternative can be eliminated.

There has been no previous study on the conceptual design of methanol production from glycerol using a graphical approach (such as CHO ternary diagrams). This study utilizes a graphical insight-based approach to convert glycerol into methanol. One of the main advantages of such insight-based approach is that one can determine the minimum amount of raw materials required to generate a product prior to a detailed design. One can also use this insight-based approach to target the amount of waste that can be generated from a given process (Patel 2007). The rest of the manuscript is structured as follows: (i) significance of CHO ternary diagrams in process design, (ii) thermodynamic equilibria in CHO ternary diagrams, (iii) presentation of glycerol reforming processes on a CHO ternary diagram and (iv) using a CHO ternary diagram to set the targets for methanol production from glycerol, (v) use these targets to develop a flowsheet for methanol production from glycerol.

## Significance of CHO Ternary Diagrams in Process Design

Most of biorefinery feedstocks consist of carbon, hydrogen and oxygen. These feedstocks can be easily represented on a carbon-hydrogen-oxygen (CHO) ternary diagram. This CHO ternary diagram is a triangular representation whereby each vertex represents a pure atom (carbon, hydrogen and oxygen). CHO ternary diagrams play a crucial role in various chemical processes such as gasification, combustion and fuel cells (Cairns and Tevebaugh 1964). Cairns and Tevebaugh (1964) have extensively used these CHO ternary diagrams to determine the equilibrium composition of different chemical species in a temperature range of 298–1500 K and at a pressure of 1 atm. Within this temperature range, the only species present in significant composition at equilibrium are  $H_2$ , CO,  $H_2O$ ,  $CO_2$ ,  $CH_4$  and C(s). The same authors used these diagrams to determine at which conditions fuel cells can operate without deposition of carbon in the same temperature range and at 1 atm. The carbon deposition boundary curves shrink with an increase in temperature until they become a straight-line joining CO and  $H_2$  at a temperature range of 1200–1500K. This implies that, at this temperature range, the dominating species are  $H_2$  and CO.

Muramoto et al. (2017) investigated the composition of fuel gas used in the solid oxide fuel cells (SOFCs) through chemical equilibrium calculations at pressures and temperatures up to 30 bars 1000 °C respectively. Results revealed that the carbon deposition region shrinks in the area rich in hydrogen and enlarges in the area rich in oxygen with

an increase in total pressure. The minimum amount of different oxidising agents (steam, oxygen and carbon dioxide) required to prevent the deposition of carbon was calculated at high pressure (30 bars). Prins et al. (2006) applied these CHO ternary diagrams so that the efficiency of wood gasification and torrefaction can be analysed whereas Ptasiniski et al. (2007) used these diagrams in order to compare the gasification process of various biofuels and coal.

Even though these works provide important guidelines in determining the operating conditions of thermochemical process (gasification), there is a lack of literature in applying these CHO ternary diagrams in process synthesis. Their focus was the modelling and representation of thermochemical process on CHO ternary diagrams.

Tay et al. (2011a) have extended the significance of these CHO ternary diagrams in process synthesis via gasification. It was shown that these CHO ternary diagrams can be used to determine the performance of an integrated biorefinery prior to a detailed design (determine the maximum amount of methanol produced from 1 ton of biomass steam gasification). However, Tay et al. (2011a) did not provide any sustainability tool in conjunction with the CHO ternary diagram to evaluate such biorefinery. Litheko (2017) extended the work of Tay et al. (2011a) by incorporating sustainability

metrics such as carbon efficiency, atom economy and E-factor.

To date, there is no study that has developed a process simulation for a biorefinery flowsheet based on targets obtained from the CHO ternary diagram. In this manuscript, CHO ternary diagrams are used to set targets and Aspen Plus uses these targets to develop an entire flowsheet for methanol synthesis from glycerol via reforming process. Figure 1 shows different steps used in this manuscript.

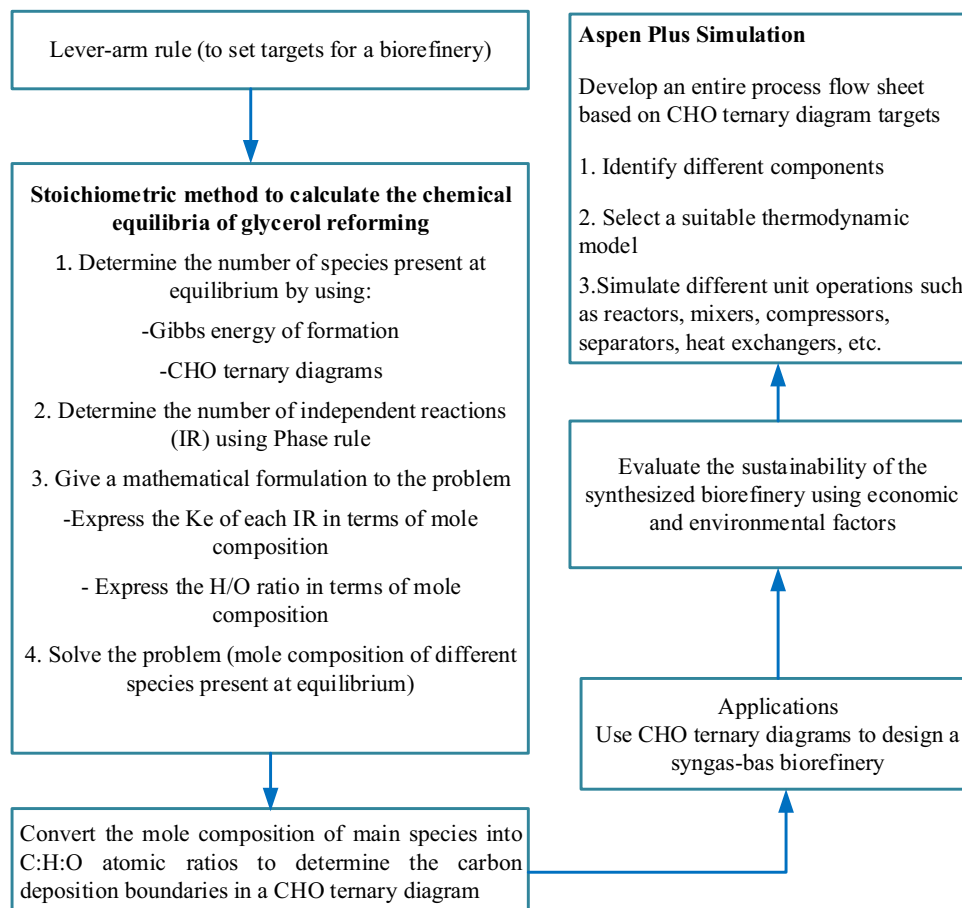
## Using CHO Ternary Diagram to Determine the Overall Material Balance

The overall process for the synthesis of 1 kmol of methanol from glycerol is given by Eq. (1). At this stage, these are the only components considered during the synthesis of methanol.



where a, b, c and d are the respective moles of  $C_3H_8O_3$ ,  $H_2O$ ,  $O_2$  and  $CO_2$

**Fig. 1** Procedure utilized for the conceptual design and simulation of a glycerol biorefinery



Equation (1) can be represented on the CHO ternary diagram to determine the overall balance as shown in Fig. 2.

Figure 2 shows the overall material balance for methanol synthesis from glycerol on the CHO ternary diagram. It is assumed that the impurities present in glycerol are insignificant and do not impact the process significantly. Pathway P<sub>1</sub> ( $a\text{C}_3\text{H}_8\text{O}_3 + c\text{O}_2 \Rightarrow 1\text{CH}_4\text{O} + d\text{CO}_2$ ) represents a region whereby water is not required nor produced during the synthesis of methanol. The lever arm rule reveals that the minimum amount of C<sub>3</sub>H<sub>8</sub>O<sub>3</sub> needed for the synthesis of 1 kmol of CH<sub>4</sub>O is 0.5 kmol. At this pathway (P<sub>1</sub>), the process uses 0.25 kmol of O<sub>2</sub> and generates 0.5 kmol CO<sub>2</sub>. Pathway P<sub>3</sub> ( $a\text{C}_3\text{H}_8\text{O}_3 + b\text{H}_2\text{O} \Rightarrow 1\text{CH}_4\text{O} + d\text{CO}_2$ ) represents a region whereby O<sub>2</sub> is not needed nor produced. The minimum amount of C<sub>3</sub>H<sub>8</sub>O<sub>3</sub> needed for the synthesis of 1 kmol of CH<sub>4</sub>O at this point is 0.4286 kmol. The process utilizes 0.2857 kmol of H<sub>2</sub>O and generates 0.2857 kmol of CO<sub>2</sub> as waste. A process that does not require or produce CO<sub>2</sub> is presented by pathway P<sub>2</sub> ( $a\text{C}_3\text{H}_8\text{O}_3 + b\text{H}_2\text{O} \Rightarrow 1\text{CH}_4\text{O} + c\text{O}_2$ ) and the minimum amount of C<sub>3</sub>H<sub>8</sub>O<sub>3</sub> needed to produce 1 kmol of CH<sub>4</sub>O is 0.333 kmol. At this pathway, the process uses 0.667 kmol of H<sub>2</sub>O and generates 0.333 kmol O<sub>2</sub>. It can be shown that, CHO ternary diagrams are used to determine the inputs and outputs for methanol synthesis of methanol from glycerol. In Fig. 2, parameter Dx represents the distance of compound  $\times$  relative to either P1, P2 or P3. For example, D<sub>CO<sub>2</sub>(2)</sub> represents the distance of CO<sub>2</sub> relative to P3.

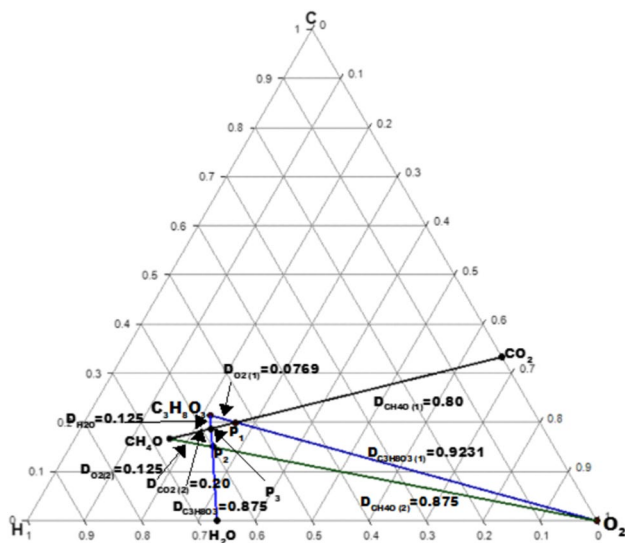


**Fig. 2** Overall mass balance target for methanol synthesis from glycerol

## Evaluating the Sustainability of a Glycerol Biorefinery

From Fig. 2, it is shown that there are three alternatives (P1:  $a\text{C}_3\text{H}_8\text{O}_3 + c\text{O}_2 \Rightarrow 1\text{CH}_4\text{O} + d\text{CO}_2$ , P2:  $a\text{C}_3\text{H}_8\text{O}_3 + b\text{H}_2\text{O} \Rightarrow 1\text{CH}_4\text{O} + c\text{O}_2$  and P3:  $a\text{C}_3\text{H}_8\text{O}_3 + b\text{H}_2\text{O} \Rightarrow 1\text{CH}_4\text{O} + d\text{CO}_2$ ) that occur within a glycerol biorefinery (methanol production from glycerol). So, it is important to evaluate its sustainability at early stage. This will not only help the process designer screen out unnecessary alternatives prior to detailed design but could also help in identifying key areas for improvement in the future. If problems are well identified at the early stage, the process designer would not spend a lot of money in handling them (Zheng et al. 2012). There are different tools that are used in evaluating a biorefinery sustainability (Zheng et al. 2012). This work only considers 5 tools namely Gibbs energy, atom economy, economic potential, carbon efficiency and E-factor. Gibbs energy is used to analyse the thermodynamic feasibility of a process. It tells the designer whether a given reaction/alternative is thermodynamically feasible or not. Equation (2i) can be used to determine the change in Gibbs energy at 298K ( $\Delta G^\circ$ ). If  $\Delta G^\circ$  is less than zero for a given alternative, then this alternative is feasible in thermodynamic point of view, and if it is higher than zero, then the alternative is not feasible. Thus, this alternative can be eliminated.

$$\Delta G^\circ = \sum n_i (\Delta G_f^\circ)_{\text{product } i} - \sum n_j (\Delta G_f^\circ)_{\text{reactant } j} \quad (2i)$$

where  $n$  and  $\Delta G_f^\circ$  the stoichiometric coefficient and change in Gibbs energy of formation (kJ/mol)

The second tool is the economic potential (EP). The process designer can calculate the profitability of each alternative by using Eq. (2ii).

$$EP = \sum n_i P_{\text{product } i} - \sum n_j P_{\text{reactant } j} \quad (2ii)$$

where  $n$  and  $P$  are the stoichiometric coefficient and price of a chemical species.

If an alternative has a negative economic potential ( $EP < 0$ ), then it is not economically feasible or profitable. But if the economic potential is positive ( $EP > 0$ ), then the alternative is deemed economically profitable.

A biorefinery sustainability can also be evaluated by calculating the atom economy of each alternative. Consider a process whereby species A is the reactant and B is the product while C is the waste. The atom economy can be calculated using Eq. (2iii)

$$\% \text{ atom economy} = \frac{bM_B}{aM_A} \times 100 \quad (2iii)$$

where  $a$  and  $b$  are the stoichiometric coefficients of A and B respectively and  $M_B$  and  $M_A$  are the respective molecular



weight of B and A. If the atom economy is high, then less waste will be generated.

Lastly, carbon efficiency (%C) and E-factor can be calculated using Eq. (2iv) and (2v) respectively (Patel 2015).

$$\%C = \frac{\text{moles of C in desired product}}{\text{moles of C in the feed}} \times 100 \quad (2iv)$$

$$\text{E-factor} = \frac{\text{mass of waste}}{\text{mass of desired product}} \quad (2v)$$

A low E-factor means that the process generates less waste, whereas a high carbon efficiency means that significant amount of raw materials is converted into product.

### Calculating the Chemical Equilibria via Stoichiometric Approach

After the process designer has evaluated all alternatives, it is now important to carry on with the synthesis of the biorefinery. It is worthy mentioning that the synthesis of methanol from glycerol is a two-step process. The first step consists of converting glycerol into syngas through reforming process. The second step uses this syngas for the synthesis of methanol. To convert glycerol into syngas via reforming process using CHO ternary diagrams, it is crucial to start by calculating the chemical equilibria in order represent glycerol reforming process on these ternary diagrams. Stoichiometric and non-stoichiometric methods can be used to predict the equilibrium composition of different species during the reforming of glycerol. This manuscript uses a stoichiometric method to compute the equilibrium composition of these species. This method plays a significant role in process synthesis because it uses chemical reactions to relate all these different species at equilibrium (Said et al. 2021). Once these chemical reactions are known, the process designer can use CHO ternary diagrams to evaluate the composition of different species at equilibrium.

Kyle (1984) points out that, when computing the composition of different species that predominate at equilibrium using stoichiometric method, four steps must be followed. These steps are (i) different species present at equilibrium (in significant composition) must be determined, (ii) use phase rule to determine the degree of freedom, number of independent components and reactions, (iii) give a mathematical formulation to the problem and (iv) solve the mathematical problem.

A process designer can use CHO ternary diagrams to determine different species that predominate at equilibrium. Cairns and Tevebaugh. (1964) divided the CHO triangle into four areas to indicate in which area a particular chemical species should be present in a significant

quantity. A detailed explanation of these different areas can be found in the supplementary material. Based on this explanation, it is shown that only 6 species are present at equilibrium in significant composition ( $H_2$ ,  $CO_2$ ,  $CO$ ,  $H_2O$ ,  $CH_4$  and solid carbon).

Since the number of chemical species are now known, it is now crucial to determine the number of independent reactions. This can be done by using Gibbs phase rule. Using this rule, the number of independent reactions (IR) is found to be 3. The degree of freedom is 3, this means that three variables can be used to define the system at equilibrium. These variables are temperature, pressure and material balance constraint  $\left(\frac{H}{O}\right)$ .

Schwenber et al. (2016) give a summary of different chemical reactions that occur during glycerol reforming. However, the Gibbs phase rule revealed that from these different reactions, only three are independent and should contain all six chemical species. In this manuscript, three equations that relate all chemical species present at equilibrium are selected. These reactions are given in the supplementary material.

These three independent reactions contain all the six chemical species that are predominant at equilibrium and hence their equilibrium composition can be calculated. Tay et al. (2011b) point out that any set of independent reactions that are used to represent the chemical species at equilibrium provide similar equilibrium composition. One can now determine the equilibrium constants ( $K_e$ ) of the three independent reactions. The equilibrium constant for each independent reaction can be expressed in terms of mole fraction of each species as shown in Eqs. (3i)–(3iii).

$$K_{e1} = \frac{X_{H_2} X_{CO_2}}{X_{H_2O} X_{CO}} \quad (3i)$$

$$K_{e2} = \frac{x_{CH_4}}{(x_{H_2})^2} \quad (3ii)$$

$$K_{e3} = \frac{x_{CO_2}}{(x_{CO})^2} \quad (3iii)$$

where  $x_{H_2}$ ,  $x_{CO}$ ,  $x_{CO_2}$ ,  $x_{H_2O}$  and  $x_{CH_4}$  are the respective mole composition of hydrogen, carbon monoxide, carbon dioxide, water as well as methane and  $K_e$  the equilibrium constant.

The equilibrium constants of all three independent reactions can be easily determined as indicated in the supplementary material (Table SM.1).

The only parameter remaining to calculate the gaseous equilibrium compositions of the different chemical species is the atomic ratio. It is known that the sum of

mole fraction of all chemical species present in a system is always 1. This is expressed by Eqs. (4i) and (4ii)

$$\sum x_i = 1 \quad (4i)$$

$$x_{\text{CH}_4} + x_{\text{CO}} + x_{\text{CO}_2} + x_{\text{H}_2\text{O}} + x_{\text{H}_2} = 1 \quad (4ii)$$

The atomic ratio  $\left(\frac{\text{H}}{\text{O}}\right)$  can be summarized as follows (Eq. (4iii))

$$\frac{\text{H}}{\text{O}} = \frac{4x_{\text{CH}_4} + 2x_{\text{H}_2\text{O}} + 2x_{\text{H}_2}}{x_{\text{CO}} + 2x_{\text{CO}_2} + x_{\text{H}_2\text{O}}} \quad (4iii)$$

where  $\frac{\text{H}}{\text{O}}$  is the hydrogen to oxygen ratio (atomic ratio).

Simultaneously solving Eqs. (3i)–(3iii), (4i) and (4ii), the equilibrium compositions of the major chemical species can be determined at this fixed atomic ratio  $\left(\frac{\text{H}}{\text{O}}\right)$ . To fully analyse the thermodynamic equilibrium of the CHO ternary diagrams, various  $\frac{\text{H}}{\text{O}}$  ratios are used as shown in the supplementary material.

## Carbon Deposition Boundaries in CHO Ternary Diagrams

One of main challenges faced by chemical process industries is the undesired formation of carbon deposition from gaseous mixtures of carbon-hydrogen-oxygen (Jaworski and Pianko-Oprych 2017). When designing a biorefinery via a thermochemical route, it is crucial to know at which conditions carbon deposition may occur. A useful way to predict the formation of carbon deposition in CHO ternary systems is by means of triangular coordinates (Cairns and Tevebaugh 1964). The ratios of the three atoms can predict whether carbon will form or not from a given feed composition. The complete combustion of methane is used to illustrate the carbon deposition boundary on a CHO ternary diagram as shown in the supplementary material.

To determine the carbon deposition boundaries inside a CHO ternary diagram at different temperatures, syngas equilibrium compositions are converted to an atomic ratio. It must be noted that Boudouard and hydrogasification reactions are the two selected reactions that describe the formation of solid carbon. Equations describing the conversion of the mole fractions into atomic ratios (C, H and O) can be found in the supplementary material.

These atomic ratios can be plotted on a CHO ternary diagram to determine the carbon deposition boundary at different temperatures. These ratios are tabulated in the supplementary material (C:H:O atomic ratios). Once the carbon deposition boundaries are determined, the process

designer can carry on with the conceptual design of glycerol biorefinery.

## Results and Discussions Based on CHO Ternary Diagrams

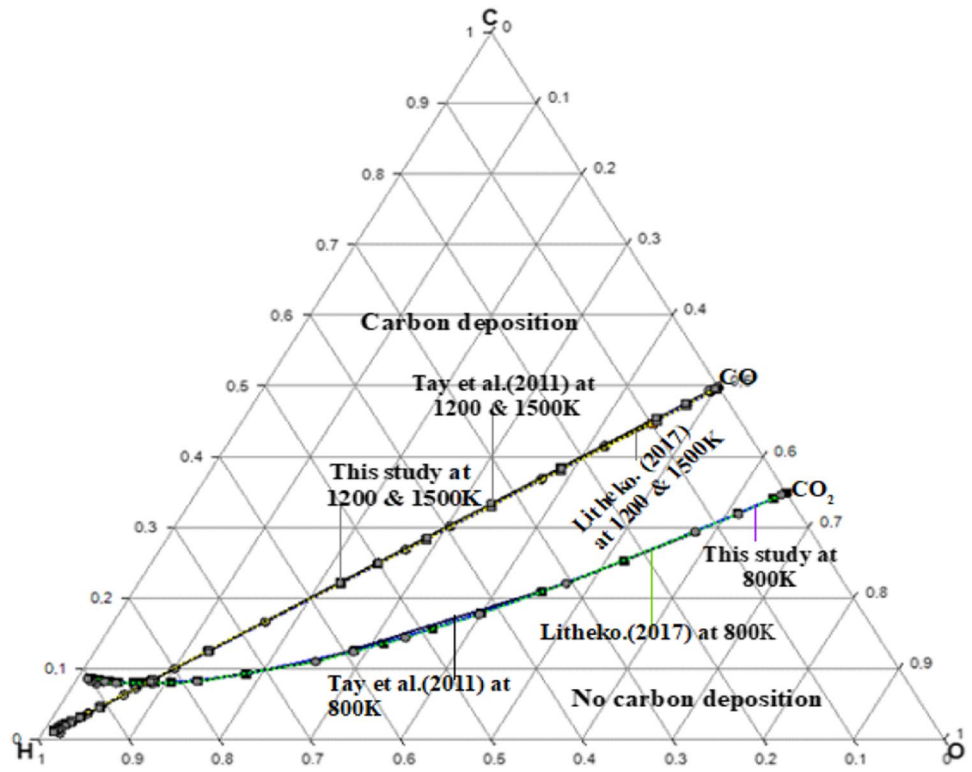
### Validation of the Stoichiometric Model

A stoichiometric equilibrium model was used to compute the gaseous compositions of five species based on three independent chemical reactions. To validate the accuracy of this model, the results computed in this work are compared with previous results from the literature. Carbon deposition boundaries generated from the current study are compared with those generated by Litheko (2017) and Tay et al. (2011a, b) at 800, 1200 and 1500K as shown in Fig. 3. It can be seen that all carbon deposition boundaries follow a similar trend at different temperatures. For example, at 800 K, the carbon boundaries are represented by a curve while at 1200 K they are shown by straight lines joining CO and H<sub>2</sub>. This simply means that, at high temperatures, H<sub>2</sub> and CO are present in significant quantity. Based on these previous studies, this model is deemed valid and sufficiently accurate to perform the conceptual design.

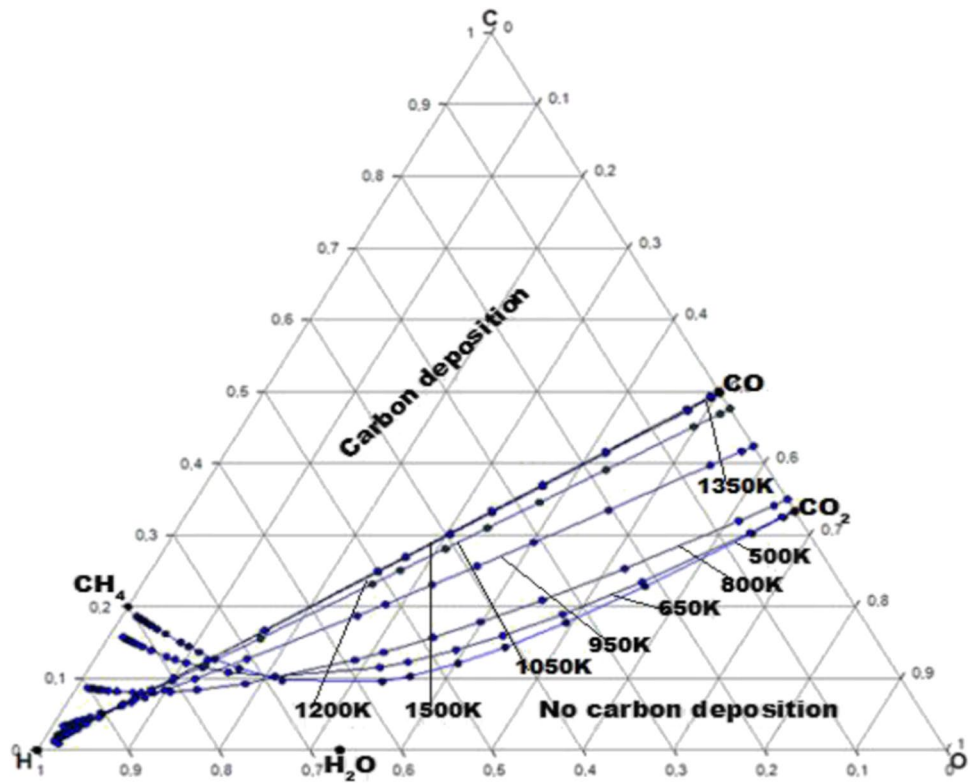
### Carbon Deposition Boundaries in a CHO Ternary Diagram

Figure 4 shows the trend of carbon deposition boundaries in a temperature range of 500–1500 K. Each point on a carbon deposition boundary at a particular temperature represents the composition of H<sub>2</sub>, CO, CO<sub>2</sub>, CH<sub>4</sub> and H<sub>2</sub>O in equilibrium with solid carbon. Above this point, the deposition of solid carbon occurs, whereas below this point there is no formation of carbon deposition. This same figure reveals other important information, and it should not be overlooked. The following can be deduced from Fig. 4: From 500 K up to 800 K, all solid carbon deposition boundaries are represented by curves while from 950 K up to 1500 K these deposition boundaries are represented by straight lines joining CO and H<sub>2</sub>. This means that, at low temperatures, CO<sub>2</sub>, CH<sub>4</sub> and H<sub>2</sub>O are the most predominant species at equilibrium. Considering the methanation and Boudouard reactions for example ( $\text{C} + 2\text{H}_2 \rightleftharpoons \text{CH}_4$  and  $2\text{CO} \rightleftharpoons \text{C} + \text{CO}_2$ ), the equilibrium of these reactions will shift to the right in order to produce more CH<sub>4</sub> and CO<sub>2</sub> at low temperatures. Increasing the temperature, carbon deposition boundaries move from CH<sub>4</sub>-CO<sub>2</sub> composition lines towards CO-H<sub>2</sub> composition lines. This indicates that the equilibrium of methanation and Boudouard reactions shift to the left at high temperatures to generate more H<sub>2</sub> and CO.

**Fig. 3** Model validation based on carbon deposition boundaries



**Fig. 4** Carbon deposition boundaries at a temperature range from 500 to 1500 K



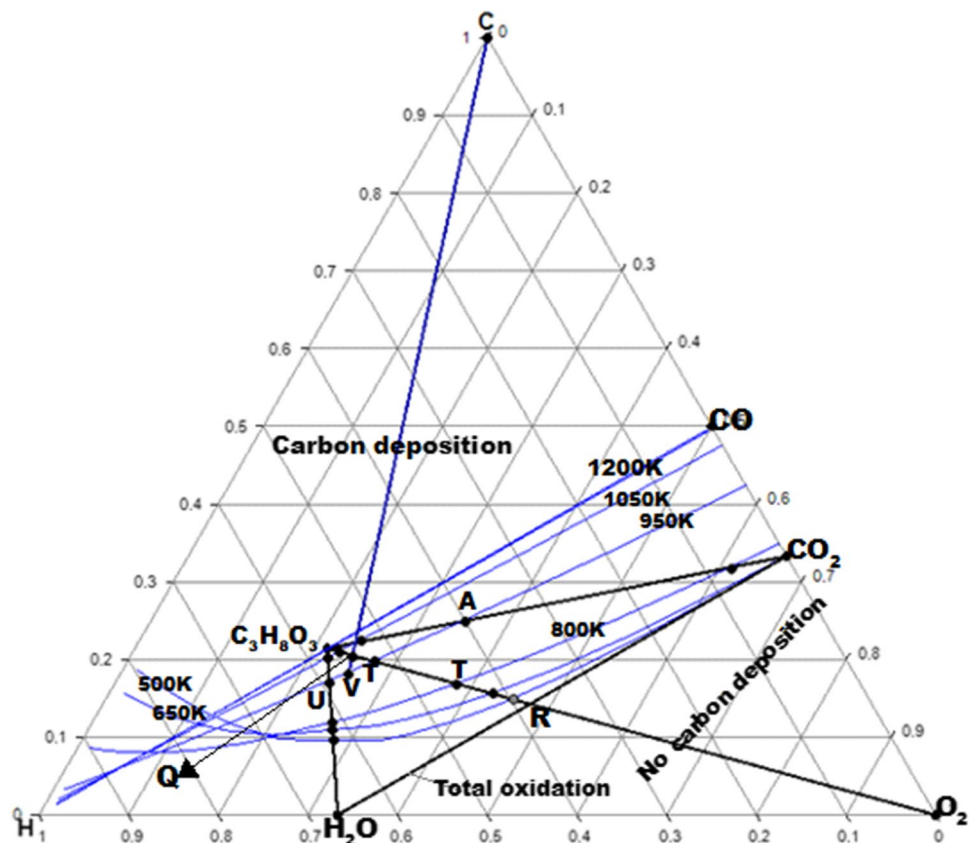


## Syngas Composition Target from Glycerol Reforming Using CHO Ternary Systems

Glycerol reforming is a process whereby glycerol is fed with another reactant commonly known as reforming agent (oxidant). The most used reforming agents are steam ( $\text{H}_2\text{O}$ ), carbon dioxide ( $\text{CO}_2$ ) and oxygen ( $\text{O}_2$ )/air or a combination of these three. Figure 5 shows the reforming of glycerol using CHO ternary diagrams at different temperatures. Line that joins  $\text{C}_3\text{H}_8\text{O}_3$  and  $\text{O}_2$  represents glycerol reforming using oxygen as reforming/oxidizing agent and this process is commonly known as glycerol partial oxidation (GPO). Glycerol steam reforming is a process whereby glycerol is fed with steam to produce syngas, this process is known as glycerol steam reforming (GSR), and it is represented by  $\text{C}_3\text{H}_8\text{O}_3$ - $\text{H}_2\text{O}$  streamline.  $\text{C}_3\text{H}_8\text{O}_3$ - $\text{CO}_2$  streamline represents glycerol reforming in the presence of carbon dioxide. This process is commonly known as glycerol dry reforming (GDR) (Roslan et al. 2020). The intersection of the boundaries with the reforming streamlines is represented by points on the diagram. These points represent the composition of syngas in equilibrium with solid carbon. For example, point U on  $\text{C}_3\text{H}_8\text{O}_3$ - $\text{H}_2\text{O}$  streamline represents syngas target composition from GSR at 950 K while the point T represents GPO at 800 K and point A shows GDR at 950 K.

**Glycerol Partial Oxidation on a Single CHO Ternary Diagram** For illustrative purposes, we consider oxygen as the oxidizing agent for the reforming of glycerol at 950 K, 1050 K and 1200 K as shown in Fig. 5. The main challenge is to know the minimum amount of  $\text{O}_2$  that will produce syngas from 1 kmol of glycerol without carbon deposition. This challenge, however, can be solved by using the lever arm rule. The carbon deposition boundaries at 950 K, 1050 K and 1200 K are also shown in Fig. 5. In the region below the carbon boundary, there is no formation of solid carbon, whereas, in the region above the boundary curve, there is a deposition of solid carbon. Figure 5 shows an arbitrary point Q with an empirical formula of  $\text{C}_{0.2111}\text{H}_{0.5428}\text{O}_{0.2461}$  ( $\frac{\text{H}}{\text{O}} = 2.2056$ ) is located above the 950 K boundary curve and on the  $\text{C}_3\text{H}_8\text{O}_3$ - $\text{O}_2$  streamline. Thus, there will be a deposition of solid carbon and the syngas composition will be targeted at point V. Point R (represents the complete combustion of  $\text{C}_3\text{H}_8\text{O}_3$ , only  $\text{H}_2\text{O}$  and  $\text{CO}_2$  are present at equilibrium) intersects the  $\text{C}_3\text{H}_8\text{O}_3$ - $\text{O}_2$  streamline and  $\text{H}_2\text{O}$ - $\text{CO}_2$  streamline. This point also lies below the carbon deposition boundary, which means that no solid carbon deposition will occur. At this point, hydrogen and carbon monoxide which are the main syngas constituents undergo a complete oxidation process (combustion) to form water and carbon dioxide according to the following reactions:  $\text{H}_2$

**Fig. 5** Glycerol reforming using CHO ternary diagrams at different temperatures



+ 0.5O<sub>2</sub> → H<sub>2</sub>O and CO + 0.5O<sub>2</sub> → CO<sub>2</sub> (Rabenstein and Hacker 2008).

To avoid complete oxidation (combustion) of hydrogen and carbon monoxide and to avoid the formation of solid carbon during the reforming of glycerol, the final product must be located at point T on carbon boundary lines. The empirical formula of this point T at 950, 1050 K and 1200 K are C<sub>0.2054</sub>H<sub>0.5245</sub>O<sub>0.2701</sub> ( $\frac{H}{O}=1.942$ ), C<sub>0.2148</sub>H<sub>0.5572</sub>O<sub>0.2279</sub> ( $\frac{H}{O}=2.445$ ) and C<sub>0.215</sub>H<sub>0.570</sub>O<sub>0.215</sub> ( $\frac{H}{O}=2.651$ ) respectively. The minimum amount of O<sub>2</sub> needed to convert 1 kmol of glycerol into syngas can now be calculated as well as the syngas composition at point T. The stoichiometric coefficients of oxygen at 950 K, 1050 K and 1200 K are calculated using the lever arm rule and are found to be 0.5741, 0.1211 and 0 respectively. These stoichiometric coefficients represent the minimum amount of O<sub>2</sub> needed to convert 1 kmol of C<sub>3</sub>H<sub>8</sub>O<sub>3</sub> into gaseous product or syngas with no carbon deposition at 950 K, 1050 K and 1200 K. The main reason that the minimum amount of O<sub>2</sub> required to convert 1 kmol of glycerol into syngas at 1200 K is zero because syngas target point at 1200 K intersects with glycerol point (this process tends to pyrolysis).

It is also important to determine the molar quantity of syngas that can be obtained at point T when 0.5741, 0.1211 and 0 kmol of O<sub>2</sub> are used to convert 1 kmol of glycerol. The empirical formulas of point T have already been determined using the CHO diagram. Using the  $\frac{H}{O}$  ratios at 950 K, 1050 K and 1200 K, the syngas composition can be interpolated from Table 2 (supplementary material).

The same reasoning is followed at different temperatures keeping in mind that point T represents the optimal composition of syngas during the reforming of glycerol with O<sub>2</sub>. Figure 6 shows syngas composition target at different temperatures. This figure indicates that at high temperatures

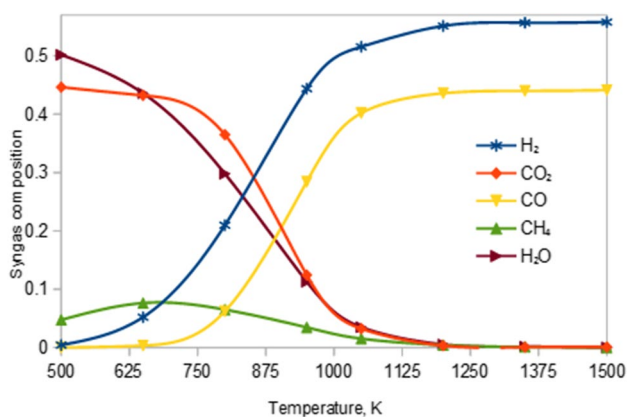


**Fig. 6** Syngas composition target from GPO by means of CHO ternary diagrams

glycerol is decomposed to form H<sub>2</sub> and CO as main constituents without forming solid carbon. For example, at 1500 K, the syngas composition from GPO is found to be 55.8% H<sub>2</sub> and 44.1% CO. These results are in agreement with the work done by Wang (2010) whereby minimization of Gibbs energy was used to study the conversion of glycerol using O<sub>2</sub> as a reforming agent and found that, at a temperature of 1500 K, the maximum mole fraction of hydrogen and carbon monoxide was found to be 57.06% and 44.55% respectively. Figure 6 shows further that the amount of methane that can be targeted from GPO without any solid carbon formation is less than 5% from 950 K up to 1500 K. Low temperatures favour the production of CO<sub>2</sub>, CH<sub>4</sub> and H<sub>2</sub>O while high temperatures favour H<sub>2</sub> and CO production (see Fig. 6). This is caused by equilibrium reactions such as Boudouard (CO+2CO<sub>2</sub> ↔ 2CO) and methanation (C+H<sub>2</sub>O ↔ CO+H<sub>2</sub>). High temperatures tend to shift the equilibrium to the right to produce more H<sub>2</sub> and CO while at low temperatures the equilibrium of these reactions tends to shift to the left to produce more H<sub>2</sub>O and CO<sub>2</sub>. For example, the amount of CO<sub>2</sub> and H<sub>2</sub>O targeted from GPO at 500 K is 44.63% and 50.18% respectively while, at 1200 K, these compositions become 0.33 % and 0.54 % respectively (CO<sub>2</sub> and H<sub>2</sub>O).

**Glycerol Steam Reforming on a Single CHO Ternary Diagram** The GSR process can be represented on the CHO ternary systems at 950 K, 1050 K and 1200 K (see Fig. 5). Point U (syngas target point) is the intersection point between C<sub>3</sub>H<sub>8</sub>O<sub>3</sub>-H<sub>2</sub>O streamline and the carbon deposition boundary curves at 950 K, 1050 K and 1200 K. The equilibrium composition of the syngas is targeted at point Q and the empirical formula of this point is C<sub>0.179046</sub>H<sub>0.588172</sub>O<sub>0.232782</sub> ( $\frac{H}{O}=2.527$ ), C<sub>0.202</sub>H<sub>0.577</sub>O<sub>0.221</sub> ( $\frac{H}{O}=2.611$ ) and C<sub>0.215</sub>H<sub>0.570</sub>O<sub>0.215</sub> ( $\frac{H}{O}=2.651$ ) at 950 K, 1050 K and 1200 K respectively. The distances of glycerol (D<sub>GL</sub>) and steam (D<sub>H2O</sub>) relative to point U are determined, and from these distances, the stoichiometric coefficient of H<sub>2</sub>O can be calculated.

The optimum amount of steam needed to convert one kmol of glycerol without carbon deposition at 950 K, 1050 K and 1200 K is calculated using the lever arm rule and found to be 5.908 and 1.199 and 0 kmol per kmol glycerol respectively. Performing a carbon balance and using Table 2 (supplementary material), the molar quantity of syngas produced at point U is 7.4437, 6.9165 and 6.8016 kmol syngas/kmol glycerol without carbon deposition at 950 K, 1050 K and 1200 K respectively.

The reforming of glycerol using steam at 500 K, 650 K, 800 K, 1350 K and 1500K is calculated in the same way and the optimal syngas composition from glycerol at different temperatures is shown in Fig. 7. This figure shows that the composition of H<sub>2</sub> and CO increases with an increase

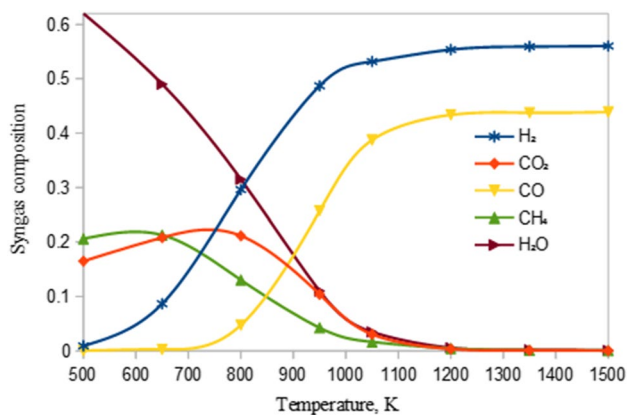


Fig. 7 Syngas composition target via GSR using CHO diagrams

in temperature until a respective maximum composition of 56.03% and 43.88% at 1500 K is reached. The composition of CH<sub>4</sub> increases from 20.61% at 500 K to 21.28% at 650 K and starts to decrease from 800 K up to 1500 K, whereas H<sub>2</sub>O composition decreases with an increase in temperature. The composition of CO<sub>2</sub> increases slightly at 500, 650 and 800 K and starts to decrease from 950 K until it reaches 0.0085% at 1500 K (see Fig. 7). Two equilibrium reactions ( can explain the variation of syngas composition from GSR): CH<sub>4</sub>+CO<sub>2</sub>↔2CO+2H<sub>2</sub> (methane dry reforming) and CO+H<sub>2</sub>O↔CO<sub>2</sub>+2H<sub>2</sub> (water gas shift reaction). At low temperatures, these reactions' equilibrium tends to shift to the left to increase the production of CH<sub>4</sub> and CO<sub>2</sub> while at high temperatures it tends to shift to the right in order to consume CH<sub>4</sub> and CO<sub>2</sub> and produce more syngas (Adhikari et al. 2007).

**Glycerol Dry Reforming on a CHO Ternary Diagram** The GDR process is considered at 950 K and 1050 K graphically by means of a CHO ternary diagram in Fig. 5. A line is drawn from glycerol to carbon dioxide and the point A is the intersection between C<sub>3</sub>H<sub>8</sub>O<sub>3</sub>-CO<sub>2</sub> streamline and carbon deposition boundary lines at 950 K and 1050 K. The empirical formulae of this point Q that represent the syngas composition target at 950 K and 1050 K are C<sub>0.250579</sub>H<sub>0.412206</sub>O<sub>0.337215</sub> and C<sub>0.2261</sub>H<sub>0.5402</sub>O<sub>0.2337</sub> respectively. The  $\frac{H}{O}$  ratios of this point at 950 K and 1050 K are 1.222 and 2.311 respectively. The composition of the syngas can be calculated by interpolation of the data provided in the supplementary material. Furthermore, the minimum amount of carbon dioxide needed to convert 1 kmol of glycerol into syngas (at point Q) at 950 K and 1050 K without carbon deposition can be determined.

The target for the syngas composition during glycerol dry reforming at 500–1500 K is calculated in the same way. Figure 8 gives a summary of GDR at different temperatures. At low temperatures glycerol dry reforming, a low composition of H<sub>2</sub> and CO is obtained but an increase in temperature

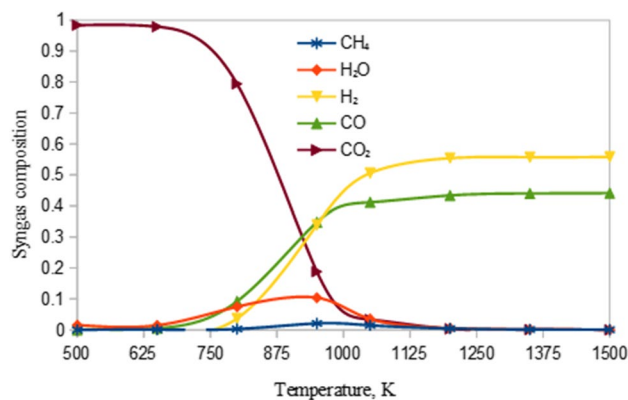


Fig. 8 Syngas composition target from glycerol dry reforming using CHO ternary systems

gives a high composition of H<sub>2</sub> and CO. The highest H<sub>2</sub> and CO composition from GDR is targeted at 55.5 % and 44.4% at 1500 K using 1 kmol of glycerol as a feed. The optimum amount of CO<sub>2</sub> required to produce this syngas composition is targeted at 0.0 kmol CO<sub>2</sub>/kmol glycerol indicating that glycerol is decomposed at this temperature.

**Effect of Temperature on Glycerol-Derived Syngas Ratio (H<sub>2</sub>:CO) via Partial Oxidation, Steam and Dry Performing Processes**

The syngas ratio (H<sub>2</sub>:CO) for the synthesis of chemicals is very crucial and most processes require a syngas ratio in the range of 1–3 (Kale and Kulkarni, 2010). For example, the synthesis of methanol from syngas requires a syngas ratio of 2.0 (Tay et al. 2011a). Figure 9 reveals that, neither steam, dry reforming nor partial oxidation of glycerol produces a syngas that can be used for the downstream applications at 800 K (syngas ratio out of range of 1–3).

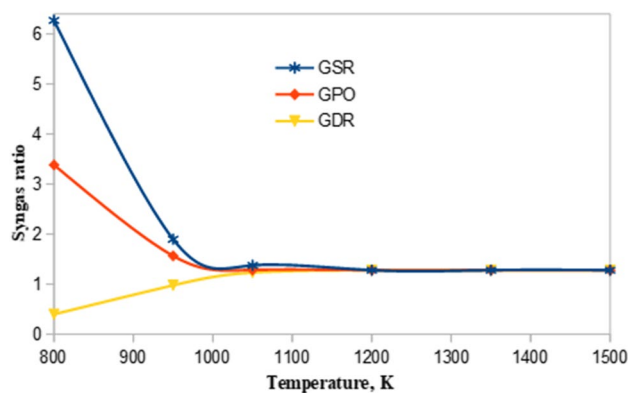


Fig. 9 Effect of temperature on glycerol-derived syngas ratio

From 950 K up to 1500 K, the syngas produced from GSR, and GPO can be used for the synthesis of various chemicals because the  $H_2:CO$  ratio falls within the range.

For example, GSR produces a syngas ratio of 1.895 at 950 K while GPO generates a  $H_2:CO$  ratio of 1.561 at the same temperature. The syngas ratio decreases with an increase in temperature for both glycerol steam reforming and partial oxidation because high temperatures favour the formation of  $H_2$  and  $CO$ . Even though the syngas ratio decreases with an increase in temperature, glycerol steam reforming and partial oxidation are still favourable for syngas production. However, this syngas does not meet the requirement for downstream applications such as methanol. This syngas ratio can be adjusted using different methods such as mixing glycerol with  $CH_4$  (using steam as a reforming agent) or using water gas shift reaction.

Figure 9 also shows that from 1050 K up to 1500 K, GDR generates a syngas ratio ( $H_2:CO$ ) that falls within the range (1–3). Therefore, this syngas could be favourable for downstream processes such as dimethyl ether or methanol. It is also interesting to see that all three reforming agents ( $H_2O$ ,  $O_2$  and  $CO_2$ ) produce same syngas ratio in a temperature range of 1200–1500 K.

## Methanol Synthesis from Glycerol Using CHO Ternary Diagrams

### Using Glycerol-Derived Syngas for Methanol Synthesis

The production of methanol from glycerol is a two-step process. The first step consists of converting glycerol into syngas while the second step utilizes the glycerol-derived syngas for methanol synthesis. The requirements for methanol synthesis from syngas are as follows:  $H_2/CO \geq 2$  ( $x_{H_2}/x_{CO} \geq 2$ ) and  $CO_2/CO \leq 0.6$  ( $x_{CO_2}/x_{CO} \leq 0.6$ ) (Tay et al. 2011a). Looking at Fig. 9, none of the three reforming agents ( $H_2O$ ,  $O_2$  and  $CO_2$ ) produces syngas that fulfil methanol synthesis specifications in terms of  $H_2/CO$ . At a temperature range of 500–1050 K, GSR produces the highest syngas ratio (see Fig. 9). At a temperature range of 1200–1500 K, all glycerol reforming processes produce the same syngas ratio because, at these temperatures, the syngas target point intersects with the glycerol point as shown in previous sections. Huang et al. (2018) have shown experimentally that introducing methane in glycerol steam reforming can produce a syngas that fulfils the methanol synthesis requirement ( $\frac{H_2}{CO} \sim 2$ ).

## Evaluating the Sustainability of Methanol from the Glycerol Process

CHO ternary diagrams (Fig. 2) have shown that there are three alternatives during the synthesis of methanol from glycerol ( $P_1$ ,  $P_2$  &  $P_3$ ). It is important to screen out any alternative that is not feasible using different tools as indicated in the “Calculating the chemical equilibria via stoichiometric approach” section. The costs and Gibbs energy of different components can be found in supplementary material.

The first step in evaluating the sustainability of each alternative is to determine the Gibbs energy. Table 1 shows that alternative  $P_2$  is not feasible from a thermodynamic point of view because its Gibbs energy is greater than zero. Therefore,  $P_2$  should be screened out. Since alternative  $P_1$  and  $P_3$  have both a negative Gibbs energy, other indicators are used in order to screen out either  $P_1$  or  $P_3$ . Comparing the atom economy of alternative  $P_1$  and  $P_3$ , it is revealed that  $P_3$  has the highest atom economy. The higher the atom economy the more sustainable an alternative (high percentage of raw materials is converted into product). This means that  $P_3$  is more sustainable than  $P_1$ . It is also shown that  $P_3$  has higher carbon efficiency and less E-factor than  $P_1$ . The evaluation of the three alternatives during the synthesis of methanol is shown in Table 1 (in terms of Gibbs energy, atom economy, carbon efficiency and E-factor).

The remaining sustainability indicator remaining to evaluate the glycerol biorefinery is the economic potential (EP). Because the price of glycerol will not remain constant once any alternative has been evaluated, it is imperative to study the effect of this price on the economic potential (alternative  $P_1$ ,  $P_2$  and  $P_3$ ) as shown in Fig. 10.

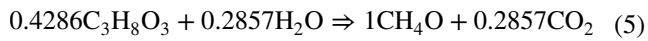
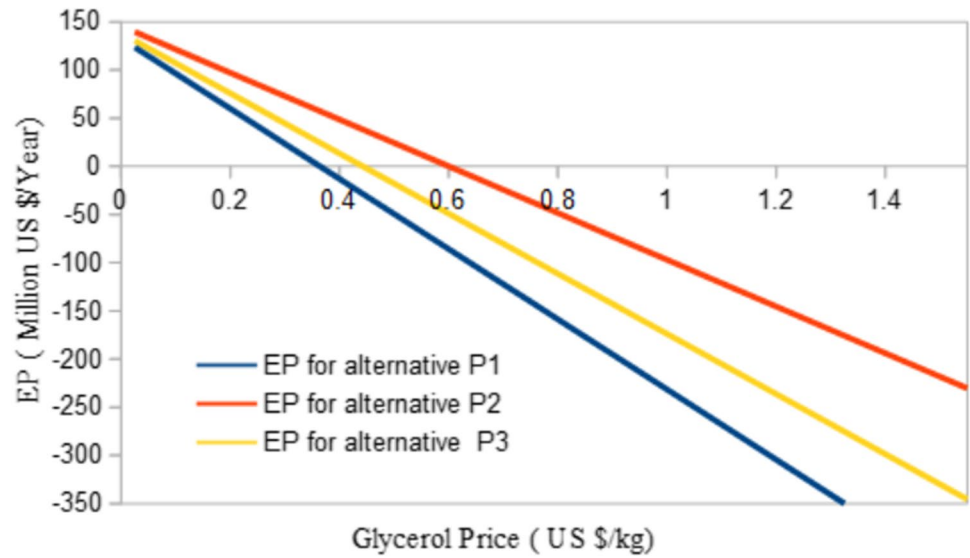
From Fig. 10, it can be seen that the price of glycerol has a significant impact on the economic potential. Comparing the economic potential of alternative  $P_1$  and  $P_3$ , it is evident to see that  $P_3$  is more feasible in a glycerol price range of \$0.025/kg–\$0.6/kg (although its EP is lower than  $P_2$ ). Taking into consideration all five sustainability indicators, the process designer can use alternative  $P_3$  for the synthesis of methanol from glycerol. The overall material target for  $CH_4O$  synthesis from  $C_3H_8O_3$  (at point  $P_3$  from Fig. 2) is summarized as follows (Eq. (5)):

**Table 1** Evaluating the sustainability of each alternative

Indicator	$P_1$	$P_2$	$P_3$
Gibbs energy, kJ/mol	– 140.56	139.29	– 20.58
Atom economy, %	59.26	75.04	71.79
Carbon efficiency, %	66.67	100	77.77
E-factor	0.687	0.333	0.393



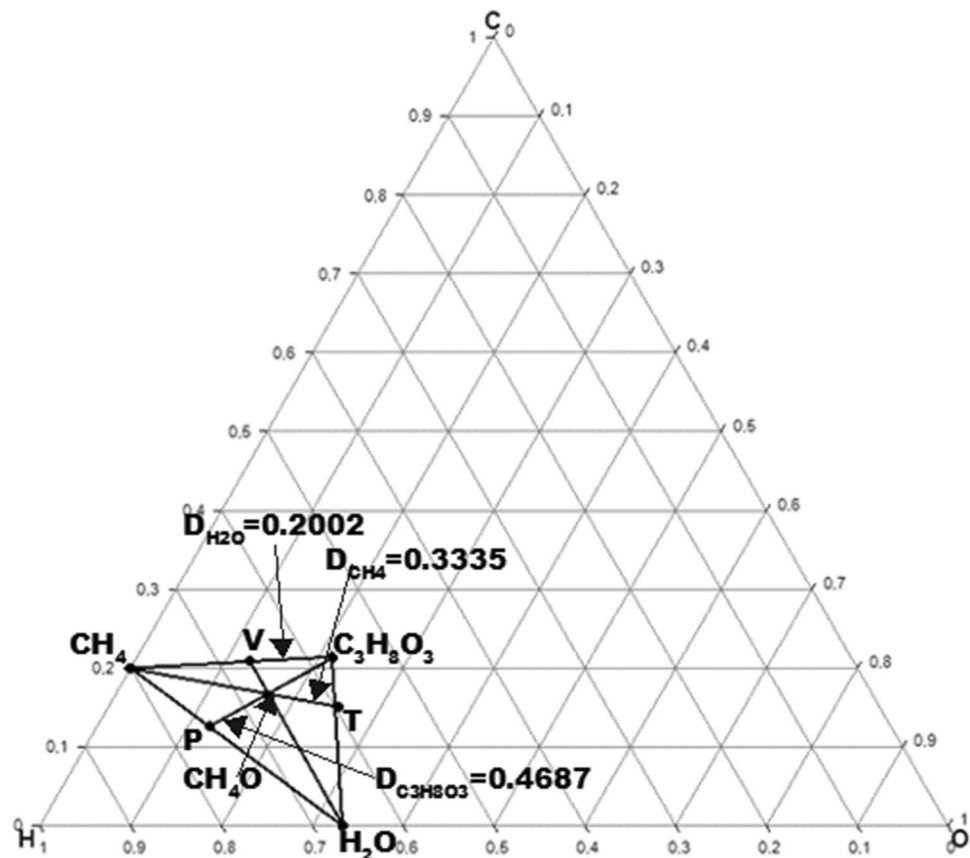
**Fig. 10** Effect of glycerol price on economic potential



In terms of mass, 1 ton of  $\text{C}_3\text{H}_8\text{O}_3$  requires 0.1304 ton of  $\text{H}_2\text{O}$  to produce 0.812 ton of  $\text{CH}_4\text{O}$  and 0.319 ton of

$\text{CO}_2$ . It must be noted that this is not a one-step process as glycerol must be converted into syngas first. In the “Methanol synthesis from glycerol using CHO ternary diagrams” section. It was shown that it is not possible to achieve this target via a two-step process.

**Fig. 11** Overall material balance for the synthesis of 1 kmol of methanol from glycerol, methane and water



### Using CHO Ternary Diagrams to Determine the Overall Mass Balance When C<sub>3</sub>H<sub>8</sub>O<sub>3</sub> Is Co-fed with CH<sub>4</sub>

Figure 11 gives a summary of mixing glycerol with methane in the presence of steam to produce 1 kmol of methanol. Point V (intersects CH<sub>4</sub>-C<sub>3</sub>H<sub>8</sub>O<sub>3</sub> streamline) is formed by drawing a line from water point to CH<sub>4</sub>-C<sub>3</sub>H<sub>8</sub>O<sub>3</sub> streamline passing through methanol point. The distance of water relative to methanol is calculated and found to be 0.2002. Point T (intersects C<sub>3</sub>H<sub>8</sub>O<sub>3</sub>-H<sub>2</sub>O streamline) is obtained by drawing a line from methane point to C<sub>3</sub>H<sub>8</sub>O<sub>3</sub>-H<sub>2</sub>O streamline passing through methanol point. The distance of methane relative to methanol is also calculated and found to be 0.3335. Lastly, point P is formed by drawing a line from glycerol point to H<sub>2</sub>O-CH<sub>4</sub> streamline passing through methanol point. The line segment from methanol to point P represents the distance of glycerol relative to methanol. This distance is calculated and found to be 0.4687. The stoichiometric coefficients of water, methane and glycerol are calculated using these different relative distances and found to be 0.4, 0.4 and 0.2 respectively.

This shows that 0.2 kmol of glycerol can be co-fed with 0.4 kmol of methane in the presence of 0.4 kmol of water to produce 1 kmol of methanol. Scaling this process up, 54.35 kmol of methanol can be produced from 10.87 kmol of glycerol. It must be noted that this is a two-step process,

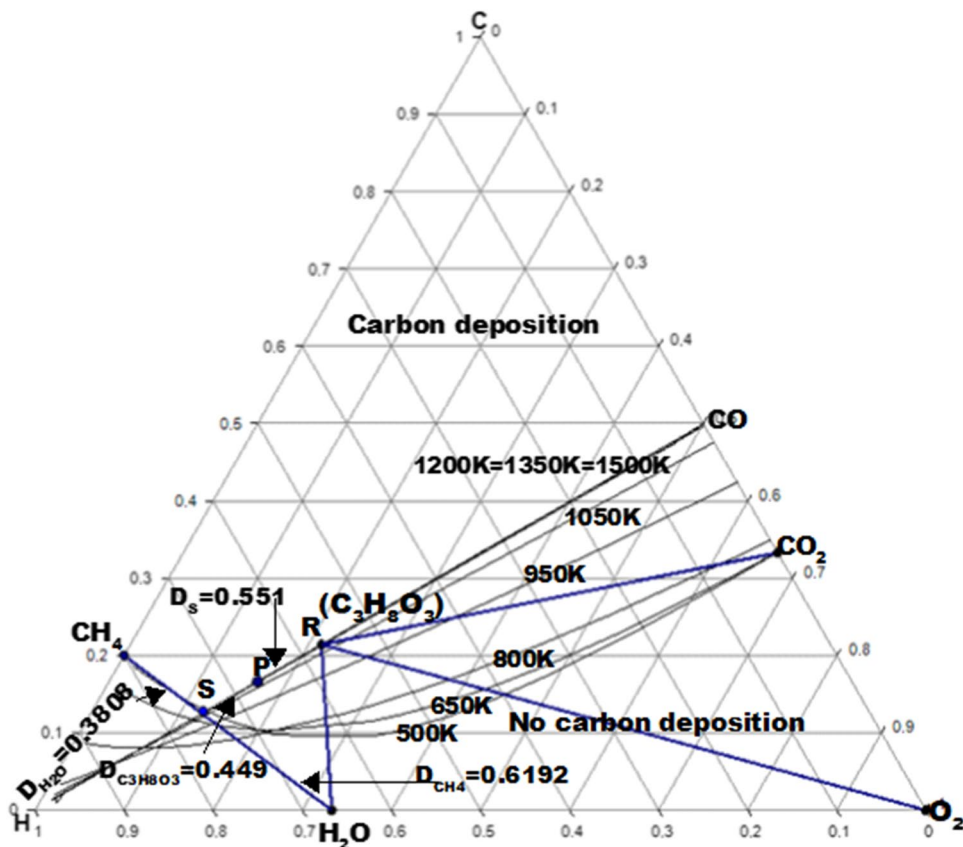
meaning that glycerol and methane should be transformed into syngas in the presence of steam and this syngas can be used to produce methanol. The next section shows this approach by means of a CHO ternary diagram.

From Fig. 12, point P represents syngas target point that fulfils the synthesis of methanol (H<sub>2</sub>: CO = 2). This point lies on carbon deposition boundary (1200, 1350 and 1500 K). Point S shows the co-feed of methane with steam, whereas point R shows GSR. Based on the same figure, it can be shown that steam is the suitable reforming agent that can be used to convert glycerol into syngas for methanol synthesis. This is because steam is closer to point P than O<sub>2</sub> and CO<sub>2</sub>. Since 1200, 1350 and 1500 K produce the same syngas composition, it is recommended to use 1200 K for

**Table 2** Glycerol-methane mixture derived syngas for methanol synthesis

Targeting point	On a molar basis (kmol)		In terms of mass (ton)	
	CO	H <sub>2</sub>	CO	H <sub>2</sub>
R	32.051	40.93	0.8974	0.08186
S	22.294	67.77	0.6242	0.1355
Total	54.345	108.70	1.5220	0.2174
H <sub>2</sub> /CO	2.00			

**Fig. 12** Glycerol reforming at different temperatures using CHO ternary diagram



the reforming of methane and glycerol mixture in order to save energy (high temperatures = high energy consumption).  $D_S$  in Fig. 12 represents the distance of point S relative to methanol (point P).

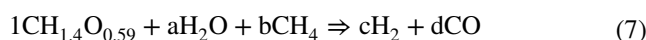
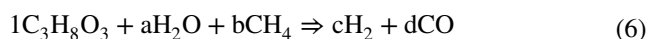
### Determining the Mixing Ratio Between Glycerol-Derived Syngas with Methane-Derived Syngas

Let  $\beta$  be the mixing ratio between methane steam reforming and glycerol-derived syngas. The lever arm rule reveals (Fig. 12) that the value of  $\beta$  is 0.551:0.449. This means that 1 kmol of glycerol-derived syngas should be mixed with 1.2272 kmol of methane-derived syngas in the presence of steam to achieve a syngas ratio of 2. The amount of syngas produced from glycerol steam reforming at 1200 K is targeted at 6.802 kmol/kmol glycerol, whereas methane steam reforming produces 8.84036 kmol/kmol methane. In term of mass, 1 ton of glycerol produces 1.0021 ton of syngas (73.938 kmol). This implies that 73.938 kmol of this glycerol-derived syngas requires 90.735 kmol from methane steam reforming derived syngas to fulfil the requirement for methanol synthesis. Table 2 gives the total amount of syngas needed for the synthesis of methanol from glycerol in the presence of methane steam co-feed. One can also determine the mixing ratio between glycerol and methane at 1200 K. Following a same reasoning as shown in Fig. 11, the mixing ratio (in terms of moles) between glycerol and methane is found to be 1:2.

### Targeting the Maximum Amount of Methanol

From Table 2, a mixture of glycerol-methane can produce 54.35 kmol of CO and 108.70 kmol of  $H_2$  for the synthesis of methanol. Figure 13 shows a simplified process for methanol synthesis from a glycerol-methane mixture. From this figure, it can be seen that the total production of methanol from 1 ton of glycerol, 0.3478 ton of methane and 0.3913 ton of steam is targeted at 1.7392 ton (based on a 100% CO conversion). Comparing the current study with Tay et al. (2011a) results, it can be shown that glycerol-methane

steam reforming produces a lower amount of methanol than biomass steam gasification/methane steam reforming. For example, considering a 50 % CO conversion, glycerol-methane reforming produces 0.870 ton of methanol, whereas biomass steam gasification/methane steam reforming produces 1.214 ton of methanol. The main reason for this difference in methanol production can be attributed to the fact that glycerol and biomass have different C:H:O atomic ratios. This means that both feedstocks (glycerol and biomass) will produce different syngas composition at the same temperature (1200 K). Another reason behind this difference is due to the fact that glycerol does not require any steam to produce syngas at 1200 K, whereas biomass requires steam. When performing an overall material balance, glycerol-methane mixture will produce less amount of methanol than a biomass-methane mixture. This comparison between the current study and Tay et al. (2011a) in terms of methanol yield is summarized in Table 3. Equations (6) and (7) show how 1 kmol of glycerol and biomass can be co-fed with methane in the presence of steam to produce a syngas that meets the requirement of methanol synthesis.

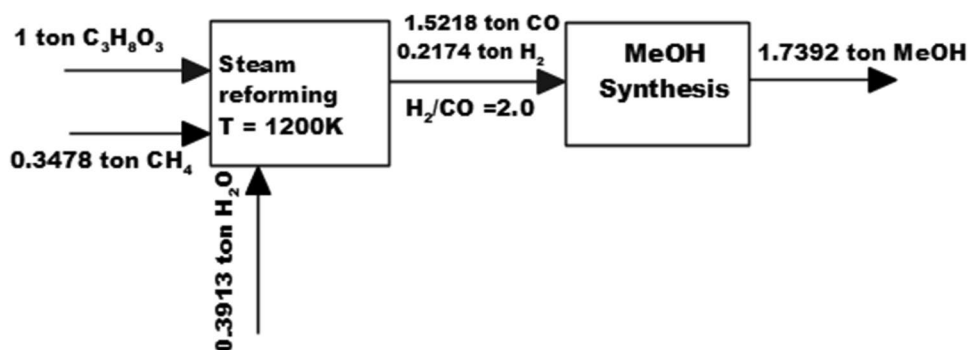


where a, b, c and d are the respective amount of  $H_2O$ ,  $CH_4$ ,  $H_2$  and CO. The algebraic solution of Eq. (6) shows that 1 kmol of glycerol can be mixed with 2 kmol of methane in the presence of 2 kmol of steam to produce 15 kmol of

**Table 3** Comparison between the current study and Tay et al. (2011a) in terms of methanol yield

Feedstock (1 ton)	Atomic ratio (C:H:O)	CO conversion (%)	Methanol yield (ton)
Biomass ( $CH_{1.4}O_{0.59}$ )	0.3344:0.4682:0.1973	50	1.214
		100	2.428
Glycerol ( $C_3H_8O_3$ )	0.2143:0.5714:0.2143	50	0.8696
		100	1.7392

**Fig. 13** Simplified block diagram for methanol synthesis from glycerol



syngas (10 kmol H<sub>2</sub> and 5 kmol CO). Solving Eq. (7), it is shown that 1 kmol of biomass can be mixed with 0.89 kmol of methane in the presence of 1.3 kmol of steam to produce 3.78 kmol H<sub>2</sub> and 1.89 kmol CO. This syngas can now be used for the synthesis of methanol.

Comparing Fig. 13 with the overall target from Eq. (5), it can be shown that introducing methane in the reformer increases syngas ratio as well as the amount of methanol.

Considering Fig. 13, the atom economy, carbon efficiency and E-factor are calculated and found to be 100%, 100% and 0 respectively. The economic potential of this process can now be calculated using Eq. (1ii). Because the price of glycerol might fluctuate, it is important to perform a sensitivity analysis as indicated in Fig. 14. Comparing the economic potential values from Fig. 14 with the values in Fig. 10 (P3), it can be seen that introducing methane in the reformer increases the overall economic potential.

The same figure (Fig. 14) shows that the approximate price of glycerol at which the economic potential is zero is

found to be \$ 0.93/kg. Table 4 gives a summary of methanol synthesis from glycerol and methane in the presence of steam.

Up to this point, it has been shown that CHO ternary diagrams can be used to set target for methanol synthesis from glycerol. To produce 1.739 ton of methanol, 1 ton of glycerol should be co-reformed with 0.348 ton of methane in the presence of 0.391 ton of steam (reforming agent). It is now important to use these targets to develop an entire flowsheet for this process by employing simulation tools such as Aspen Plus.

**Fig. 14** Effect of glycerol on economic potential during the synthesis of methanol

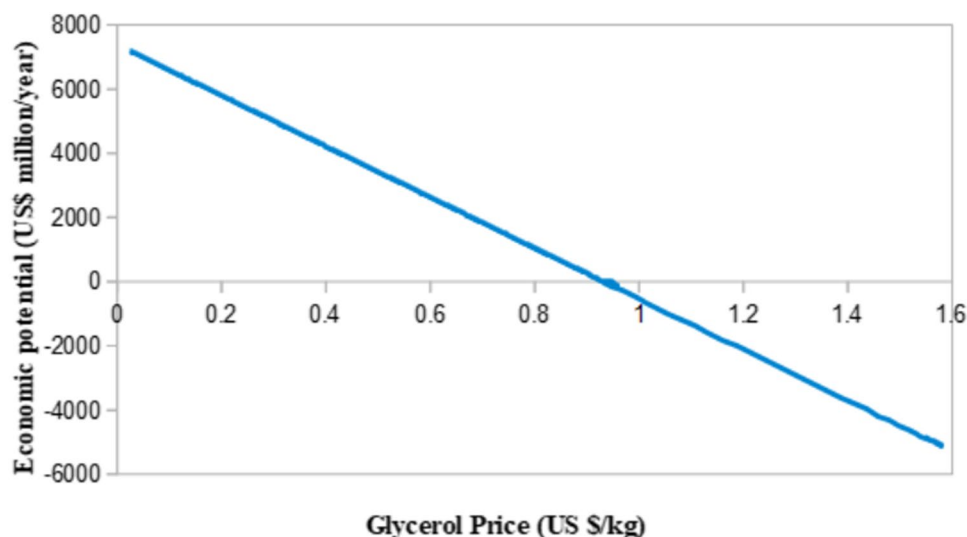


**Table 4** Summary of methanol synthesis from glycerol

Methanol biorefinery

Overall process	Reforming stage	Methanol synthesis stage
<b>Feed</b>	<b>Feed</b>	<b>Feed</b>
Glycerol: 1 ton	Glycerol: 1 ton	CO: 1.522 ton
CH <sub>4</sub> : 0.3478	CH <sub>4</sub> : 0.3478 ton	H <sub>2</sub> : 0.217 ton
CH <sub>4</sub> /glycerol ratio (mole) 2:1	<b>Operating conditions</b>	<b>Product</b>
H <sub>2</sub> O: 0.391	Temperature: 1200 K	Methanol: 1.739 ton
<b>Products</b>	Pressure: 1 bar	<b>Sustainability evaluation based on the overall process</b>
Methanol: 1.739	<b>Reforming agent</b>	Atom economy: 100%
	H <sub>2</sub> O: 0.391 ton	Carbon efficiency: 100%
	<b>Product: syngas</b>	E-factor: 0.0
	CO: 1.522 ton	Approximate economic potential at a glycerol price range of \$0.025/kg–\$0.90/kg:
	H <sub>2</sub> : 0.217 ton	\$7169.12–\$239.12 mil/annum
		Economic potential at glycerol price of \$ 0.93014/kg: 0



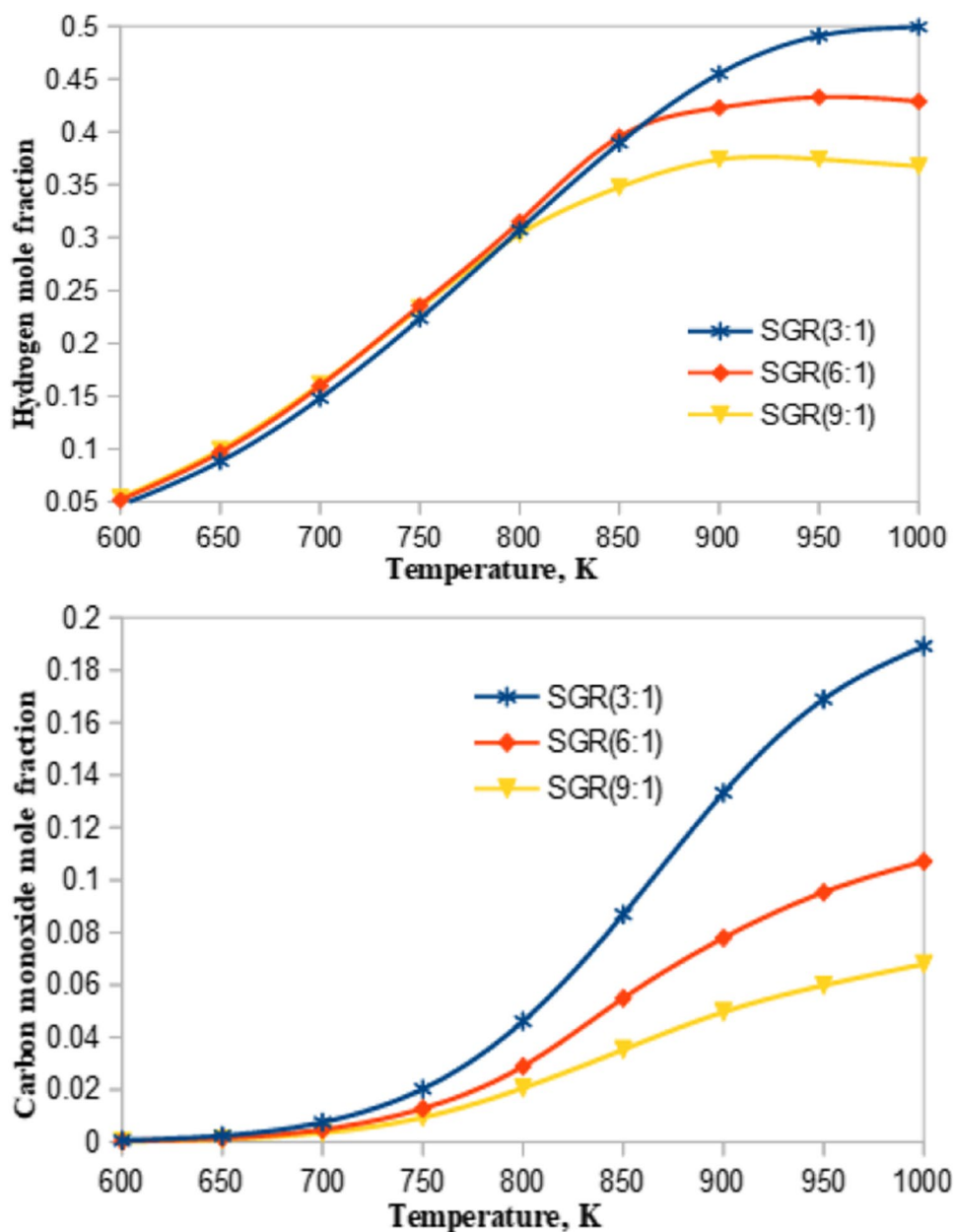
## Using CHO Ternary Diagram Targets to Develop a Flowsheet for Methanol Production in Aspen Plus

### Thermodynamic Model

It was shown that CHO ternary diagrams play a crucial role in determining the performance of a process. In other words, these diagrams assist in determining the amount of raw materials required for the synthesis of a specific product. Once the overall process target is known, the process designer can develop an entire process flowsheet using different simulation tools such as Aspen Plus. The most

crucial step during the simulation of any chemical process is the selection of a suitable thermodynamic model. This study uses Peng–Robinson as the thermodynamic model during the simulation of glycerol biorefinery in Aspen Plus. This model is advantageous for chemical processes that require high pressures (Carlson 1996). An example of such processes is the synthesis of methanol from syngas (50–100 bars) (Mevawala et al. 2017). Besides pressure, the polarity and non-polarity can also be used to select a thermodynamic model. Polarity is used to determine the molecular interactions between compounds. Even if a system is made of one polar molecule and the rest non-polar, it is still considered as a polar system (Chaves et al. 2016). Using the decision tree adopted from Carlson (1996), a

**Fig. 15** Model validation in terms of H<sub>2</sub> and CO mole fraction



polar (non-electrolytic compounds) path was followed. The accuracy of this model will be validated in next sections using data from (Adhikari et al. 2007). The process description as well as the Aspen flowsheet for methanol synthesis from glycerol can be found in the supplementary material.

### Reformer Model Validation

Glycerol steam reforming is used to check the accuracy of the thermodynamic model applied in Aspen Plus for the reforming stage. The operating conditions such as temperature and steam to glycerol ratios (SGRs) are taken from (Adhikari et al. 2007). Figure 15 shows the effect of temperature and steam to glycerol ratio (SGR) on hydrogen mole fraction at 1 bar. Low SGR and high temperature favour the production of hydrogen. For example, at 950 K and at an SGR of 3:1, the mole fraction of hydrogen is found to be approximately 48%, whereas an SGR of 6:1 at 950 K produces approximately 43% of hydrogen. The trend of hydrogen mole fraction at different temperatures and SGRs corroborates with Adhikari et al. (2007). Adhikari et al. (2007) showed that a high mole fraction of hydrogen is produced at high temperatures and low SGRs. The same figure also shows that both temperature and SGR have a significant impact on carbon monoxide mole fraction. For example, at 950 K and an SGR of 3:1, the mole composition of carbon monoxide is found to be approximately 17%, whereas at 950 K and an SGR of 6:1, carbon monoxide mole fraction is reduced to approximately 10%. Therefore, this thermodynamic model is deemed valid and can be used to convert the mixture of glycerol-methane into syngas in the presence of steam.

### Methanol Synthesis Reactor Model Validation

This section focuses on the validation of methanol synthesis reactor based on the Langmuir-Hinshelwood-Hougen-Waston (LHHW) method. To check the accuracy of methanol synthesis from glycerol and methane mixture in the presence of steam, feed flowrate from (Zhang et al. 2020) (32.1 kmol/h of  $H_2$ , 13.786 kmol/h of CO, 1.141 kmol/h of  $CO_2$  and 0.175 kmol/h of  $CH_4$ ) was used as an input to the simulation. The flow rate of methanol in this study was found to be 7.9 kmol/h while Zhang et al. (2020) found a molar flow rate of 8.04 kmol/h. The percentage error between these two results is roughly 1.74%. The reason behind this error can be attributed to the kinetic model that is used in the simulation. In this study, the adsorption expression has 4 terms, whereas Zhang et al. (2020) used 2 terms. Zhang et al. (2020) did not specify the thermodynamic used in the simulation and this can also contribute to the difference. Therefore, the model proposed is deemed valid and can be

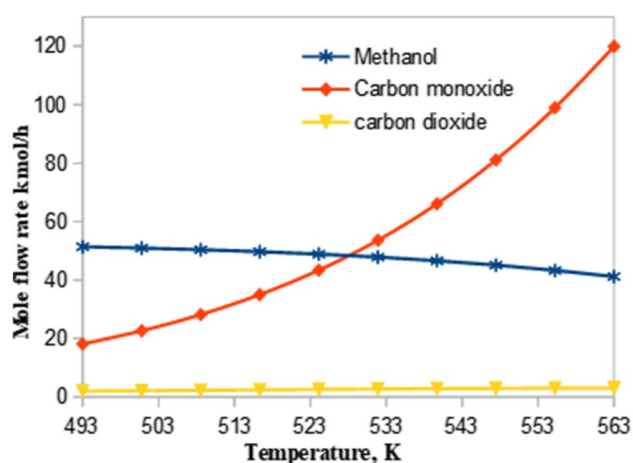


Fig. 16 Effect of plug flow reactor temperature on methanol synthesis

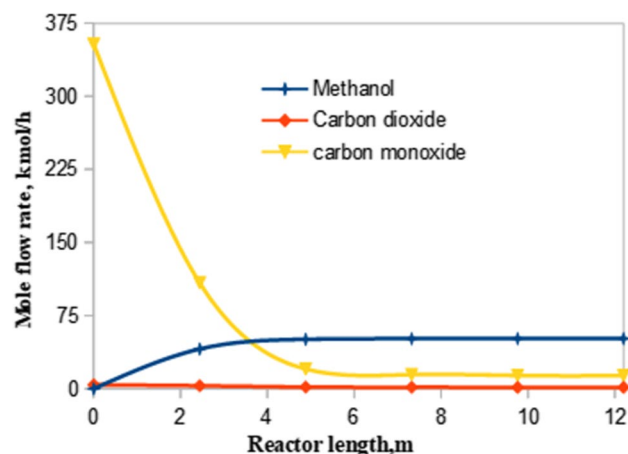


Fig. 17 Effect of plug flow reactor length on methanol synthesis

used for the synthesis of methanol from glycerol. The material balance during the synthesis of methanol from glycerol can be found in the supplementary material.

### Sensitivity Analysis

Operating conditions such as pressure and temperature play a crucial role during the synthesis of methanol from syngas. A temperature and pressure range of 493–563 K and 50–100 bar respectively is required during the synthesis of methanol. Increasing the reactor temperature can damage the catalyst while low temperatures reduce the reaction rate (Gutiérrez Ortiz et al. 2013). Taking these operating conditions into consideration, a pressure of 55 bar is selected to study the effect of plug flow reactor temperature (493–563 K) on methanol synthesis (see Fig. 16).

It can be shown from Fig. 16 that an increase in temperature decreases the molar flow rate of methanol but decreases

the conversion of carbon monoxide. It can further be shown that a temperature of 493 K produces the highest molar flow rate of methanol (approximately 51.60 kmol/h). Therefore, 493 K is an optimal temperature for methanol synthesis at a fixed pressure of 55 bar. Puig-Gamero et al. (2018) used a pine-derived syngas for the synthesis of methanol. It was shown that at a fixed pressure of 55 bar, a temperature of 493 K produced a high yield of methanol (32 kg/h).

It is also important to study the effect of plug flow reactor length on methanol production as indicated in Fig. 17. The reactor maximum length was assumed to be 12.2 m (Luyben 2010). It can be shown that methanol flow rate approximately increases from 0.007 to 50 kmol/h in a reactor length range of 0–4.9 m. From 4.9 to 12.2 m, methanol flow rate increases slightly. The same figure shows that the mole flow rate of CO increases with an increase in reactor length.

## Comparison Between CHO Ternary Diagrams and Aspen Plus for Methanol Synthesis

CHO ternary diagrams played a crucial role in setting targets for methanol synthesis from glycerol. It was shown that 1 ton of glycerol requires 0.348 and 0.391 ton of CH<sub>4</sub> and H<sub>2</sub>O respectively to produce 1.739 ton of methanol (maximum

methanol production). These inputs were now used in Aspen Plus to develop the entire flowsheet for methanol synthesis from glycerol. Table 5 gives a summary of Aspen Plus and CHO ternary diagrams results during the synthesis of methanol from glycerol. The percentage error between CHO ternary diagrams and Aspen Plus is below 2.5% (reforming stage) and approximately less than 5% (methanol synthesis). The reason behind this percentage error can be due to:

- During the synthesis of methanol via CHO ternary diagrams, it was assumed that all syngas (H<sub>2</sub> & CO) is converted into methanol (100 % conversion). In Aspen Plus, it was observed that all syngas was not converted into methanol as certain amount of this it was lost in the purge stream. The main purpose of this purge stream was to remove methane which is considered as an inert material. The amount of syngas and methane in this purge stream was found to be 7.412 kmol/h (26.90% CO & 73.10 % H<sub>2</sub>) and 0.453 kmol/h respectively. The Aspen Plus syngas overall conversion was found to be approximately 79% (due to the purge stream). This purge stream also reduced the carbon efficiency as well as atom economy.
- During the stoichiometric calculation, it was assumed that all chemical species at equilibrium follow an ideal gas behaviour, whereas in Aspen Plus simulation an equation of state was used.

**Table 5** Comparison between CHO ternary diagrams and Aspen Plus during the synthesis of methanol

Aspen Plus simulation	CHO ternary diagrams
<b>Reforming stage</b>	
<b>Inputs</b>	<b>Inputs</b>
Glycerol: 1 ton	Glycerol: 1 ton
Methane: 0.3478 ton	Methane: 0.3478 ton
Steam: 0.3913 ton	Steam: 0.3913 ton
<b>Outputs (main species)</b>	<b>Outputs (main species)</b>
H <sub>2</sub> : 0.216 ton	H <sub>2</sub> : 0.217 ton
CO: 1.486 ton	CO: 1.522 ton
H <sub>2</sub> /CO (molar ratio) = 2.02	H <sub>2</sub> /CO (molar ratio) = 2.0
<b>Operating conditions:</b>	<b>Operating conditions:</b>
Temperature: 1200 K	Temperature: 1200 K
Pressure: 1 bar	Pressure: 1 bar
<b>Methanol synthesis stage</b>	
<b>Inputs (major species)</b>	<b>Inputs (major species)</b>
H <sub>2</sub> : 0.216 ton	H <sub>2</sub> : 0.217 ton
CO: 1.486 ton	CO: 1.522 ton
<b>Outputs (major species)</b>	<b>Outputs</b>
CH <sub>4</sub> O: 1.651 ton	CH <sub>4</sub> O: 1.739 ton
CO: 0.374 ton	CO: none
H <sub>2</sub> : 0.0730 ton	H <sub>2</sub> : none
<b>Operating conditions</b>	<b>Operating conditions</b>
Temperature: 493 K	Temperature: none
Pressure: 55 bar	Pressure: none
<b>Sustainability evaluation (metrics)</b>	
Atom economy: 94.96%	Atom economy: 100%
Carbon efficiency: 95%	Carbon efficiency: 100%

It can be shown that results from CHO ternary diagrams collaborate with Aspen Plus results as the percentage error is not significant (less than 2.5% for reforming stage and less than 5% for methanol synthesis stage). Furthermore, Aspen Plus simulation does not exceed the limit set by CHO ternary diagrams in terms of methanol production. Therefore, CHO ternary diagrams are adequate tools for the conceptual and targeting for integrated biorefineries prior to a detailed design.

## Conclusions

This study intended to valorize glycerol by using it as a biorefinery feedstock for methanol synthesis. Because glycerol only consists of carbon, hydrogen and oxygen, it was shown that this compound can be plotted on CHO ternary diagrams as a single point. These CHO ternary diagrams were used to synthesize and evaluate the performance of methanol synthesis from glycerol prior to a detailed design. It was found that it is possible to use glycerol-derived syngas for the synthesis of methanol and this methanol can still be used in the production of biodiesel. This indicates that glycerol biorefinery is a good promoter of circular (bio) economy. CHO ternary diagrams revealed

that 1 ton of glycerol can be co-reformed with 0.348 ton of methane in the presence of 0.391 ton of steam to produce 1.522 ton of CO and 0.217 ton of H<sub>2</sub>. This syngas was utilized to produce 1.739 ton of methanol (based on 100 % conversion of CO). The sustainability of methanol synthesis from glycerol was evaluated using different tools such as economic potential, carbon efficiency, atom economy and E-factor. A sensitivity analysis was conducted to study the effect of glycerol price on the economic potential during the synthesis of methanol. It was found that the economic potential decreases with an increase in glycerol price. The glycerol price range that generated a positive economic potential was found to be \$0.025/kg–\$0.90/kg. At this glycerol price range, the approximate economic potential of the entire process was found to be \$7169.12 to 239.12\$ million per year. At a glycerol price of \$0.93014/kg, the process economic potential was found to be zero. The carbon efficiency, atom economy and E-factor were calculated and found to be 100%, 100 % and 0 respectively. This showed that all the syngas was converted into product with no waste generated.

CHO ternary diagram targets were used to develop an entire flowsheet for methanol synthesis from glycerol and methane using Aspen Plus simulation software. A quick sensitivity analysis was performed to study the effect of reactor temperature at a fixed pressure (55 bars). It was shown that an increase in temperature decreases methanol flow rate. The maximum methanol flow rate was achieved at a temperature of 493 K (51.539 kmol/h). The carbon efficiency and atom economy were found to be 95 and 94.96 % respectively. It was further revealed that Aspen Plus could not exceed targets set by CHO ternary diagrams (in terms of methanol production, carbon efficiency and atom economy). This manuscript only considered using targets set by CHO ternary diagrams to develop an entire Aspen flowsheet for the synthesis of methanol from glycerol. Further research should be conducted to develop aggregated methods that can be used for the conceptual design and targeting purposes.

**Supplementary Information** The online version contains supplementary material available at <https://doi.org/10.1007/s41660-022-00275-x>.

**Acknowledgements** The authors express their gratitude to the University of South Africa (UNISA) for the financial support.

**Author Contribution** Conceptualization, methodology, original draft and writing: B M. Mukeru; conceptualization, supervision, review, editing and proofreading: B. Patel.

**Data Availability** The datasets generated during and/or analysed during the current study are available in the article or in the supplementary information file. All other relevant datasets are available from the corresponding author on reasonable request.

## Declarations

**Competing Interests** The authors declare no competing interests.

## References

- Adhikari S, Fernando S, Gwaltney SR, To SDF, Bricka RM (2007) A thermodynamic analysis of hydrogen production by steam reforming of glycerol. *Int J Hydrogen Energy* 32:2875–2880. <https://doi.org/10.1016/j.ijhydene.2007.03.023>
- Asri NP (2018) Alumina supported zinc oxide catalyst for production of biodiesel from kesambi oil and optimization to achieve highest yields of biodiesel. *Euro-Mediterr J Environ Integ* 3(1):1–7. <https://doi.org/10.1007/s41207-017-0043-8>
- Bagnato G, Iulianelli A, Sanna A, Basile A (2017) Glycerol production and transformation: a critical review with particular emphasis on glycerol reforming reaction for producing hydrogen in conventional and membrane reactors. *Membranes* 7(2):1–31. <https://doi.org/10.3390/membranes7020017>
- BP. 2020 ‘BP Statistical Review of World Energy June 2020. [https://www.bp.com/Statistical review](https://www.bp.com/Statistical%20review) [Accessed 25 May 2021].
- Cairns EJ, Tevebaugh AD (1964) CHO gas phase compositions in equilibrium with carbon, and carbon deposition boundaries at one atmosphere. *J. Chem. Eng. Data* 9(3):453–462. <https://doi.org/10.1021/je60022a052>
- Carlson EC (1996) Do not gamble with physical properties for simulation. *Chem. Eng. Prog* 92:35–46
- Chaves IDG, Lopez JRG, Zapata JLG, Robayo AL, Nino GR (2016) Process analysis and simulation in chemical engineering. Springer, Cham Heidelberg, New York Dordrecht, London
- EU, 2009, Directive 2009/28/EC of the European Parliament and of the Council of 23 April 2009 on the promotion of the use of energy from renewable sources and amending and subsequently repealing Directives 2001/77/EC and 2003/30/EC. Accessed on 8 August 2021
- EU, 2018, Directive (EU) 2018/2001 of the European Parliament and of the Council of 11 December 2018 on the promotion of the use of energy from renewable sources. [Accessed on 8 August 2021]
- Dang TNG, Sahraei OA, Illiula MC (2022) Effect of impurities on glycerol steam reforming over Ni-promoted metallurgical waste driven catalyst. *International Journal of Hydrogen Energy* 47(7):4614–4630. <https://doi.org/10.1016/j.ijhydene.2021.11.089>
- D’Avino L, Rizzuto G, Guerrini S, Sciacaluga M, Pagnotta E, Lazzeri L (2015) Environmental implications of crude glycerin used in special products for the metalworking industry and in biodegradable mulching films. *Ind Crop Prod* 75:29–35. <https://doi.org/10.1016/j.indcrop.2015.02.043>
- Fan X, Burton R, Zhou Y (2010) Glycerol (byproduct of biodiesel production) as a source for fuels and chemicals - Mini review. *Open Fuels and Energy Science Journal* 3:17–22. <https://doi.org/10.2174/1876973X01003010017>
- Freitas AC, Guirardello R (2014) Comparison of several glycerol reforming methods for hydrogen and syngas production using Gibbs energy minimization. *Int J Hydrogen Energy* 39:17969–17984. <https://doi.org/10.1016/j.ijhydene.2014.03.130>
- Gutiérrez Ortiz FJ, Serrera A, Galera S, Ollero P (2013) Methanol synthesis from syngas obtained by Supercritical water reforming of glycerol. *Fuel* 105:739–751. <https://doi.org/10.1016/j.fuel.2012.09.073>
- Harabi M, Bouguerra SN, Marrakchi F, Chryssikou LP (2019) Biodiesel and crude glycerol from waste frying oil: production, characterization and evaluation of biodiesel oxidative stability



- with diesel blends. *Sustainability* 11:1–15. <https://doi.org/10.3390/su11071937>
- Huang C, Xu C, Wang B, Hu X, Li J, Liu J, Li C (2018) High production of syngas from catalytic steam reforming of biomass glycerol in the presence of methane. *Biomass and Bioenergy* 119:173–178. <https://doi.org/10.1016/j.biombioe.2018.05.006>
- Hunpinyo P, Narataruksa P (2016) Process simulation and costing study for the FT-liquid fuel production from steam glycerol reforming. *CET* 52:241–246. <https://doi.org/10.3303/CET1652041>
- IEA, 2012b. Bio-based chemicals: value added products from biorefineries. Report for IEA.Biorefinery- Task 42. International Energy Agency (IEA), Paris,France [Accessed on 8 August 2021].
- Jaworski Z, Pianko-Oprych P (2017) On thermodynamic equilibrium of carbon deposition from gaseous C-H-O mixtures: updating for nanotubes. *Rev Chem Eng* 33(3):217–235. <https://doi.org/10.1515/revce-2016-0022>
- Kale GR, Kulkarni BD (2010) Thermodynamic analysis of dry autothermal reforming of glycerol. *Fuel Process Technol* 91:520–530. <https://doi.org/10.1016/j.fuproc.2009.12.015>
- Kaur J, Sarma AK, Jha MK, Gera P (2020) Valorisation of crude glycerol to value-added products : perspectives of process technology, economics and environmental issues. *Biotechnol Rep* 27:1–23. <https://doi.org/10.1016/j.btre.2020.e00487>
- Kousoulidou M, Fontaras G, Ntziachristos L, Samaras Z (2010) Biodiesel blend effects on a common-rail diesel combustion and emissions. *Fuel* 89:3442–3449. <https://doi.org/10.1016/j.fuel.2010.06.034>
- Kyle, B.G . (1984) *Chemical and process thermodynamics*. Third edit. Edited by B. Goodwin. Englewood cliffs, NJ: Prentice-Hall.
- Litheko, L. A. (2017) *Conceptual design of gasification-based biorefineries using the C-H-O ternary diagrams*. University of South Africa, Pretoria. <http://hdl.handle.net/10500/24350>
- Luyben WL (2010) Design and control of a methanol reactor/column process. *Ind Eng Chem Res* 49:6150–6163. <https://doi.org/10.1021/ie100323d>
- Mahabir J, Koylass N, Samaroo N, Narine K, Ward K (2021) Towards resource circular biodiesel production through glycerol upcycling. *Energy Conversion Manag* 233:113930. <https://doi.org/10.1016/j.enconman.2021.113930>
- Mevawala C, Jiang Y, Bhattacharya D (2017) Plant-wide modeling and analysis of the shale gas to dimethyl ether (DME) process via direct and indirect synthesis routes. *Appl Energy* 204:163–180. <https://doi.org/10.1016/j.apenergy.2017.06.085>
- Muramoto A, Kikuchi Y, Tachikawa Y, Lyth SM, Shiratori Y, Taniguchi S, Sasaki K (2017) High-pressure C-H-O diagrams: fuel composition, carbon deposition, and open circuit voltage of pressurized SOFCs. *Int J Hydrogen Energy* 42(52):30769–30786. <https://doi.org/10.1016/j.ijhydene.2017.10.122>
- Murillo S, Miguez JL, Porteiro J, Granada E, Moran JC (2007) Performance and exhaust emissions in the use of biodiesel in outboard diesel engines. *Fuel* 86(12–13):1765–1771. <https://doi.org/10.1016/j.fuel.2006.11.031>
- OECD FAO (2021) *OECD-FAO Agricultural Outlook 2021–2030*. OECD Publishing, Paris
- Patel B (2007) *Fundamental targets for the synthesis and evaluation of chemical processes*. University of Witwatersrand, Johannesburg
- Patel, B. (2015) ‘A thermodynamic targeting approach for the synthesis of sustainable biorefineries’, in *12th International Symposium on Process Systems Engineering and 25th European Symposium on Computer Aided Process Engineering, 31 May-4 June, Copenhagen, Denmark*, pp. 1283–1288. <https://doi.org/10.1016/B978-0-444-63577-8.50059-0>
- Plácido J, Capareda S (2016) Conversion of residues and by-products from the biodiesel industry into value-added products. *Bioresour Bioprocess* 3(1):1–12. <https://doi.org/10.1186/s40643-016-0100-1>
- Pradhan A, Mbohwa C (2014) Development of biofuels in South Africa: challenges and opportunities. *Renew Sustain Energy Rev* 39:1089–1100. <https://doi.org/10.1016/j.rser.2014.07.131>
- Prins MJ, Ptasiniski KJ, Jansens FJ (2006) More efficient biomass gasification via torrefaction. *Energy* 31(1):3458–34570. <https://doi.org/10.1016/j.energy.2006.03.008>
- Ptasinski KJ, Prins MJ, Pierik A (2007) Exergetic evaluation of biomass gasification. *Energy* 32(1):568–574. <https://doi.org/10.1016/j.energy.2006.06.024>
- Puig-Gamero M, Argudo-Santamaria J, Valverde JL, Sanchez P, Sanchez-Silva L (2018) Three integrated process simulation using aspen plus: Pine gasification, syngas cleaning and methanol synthesis. *Energy Conversion Manag* 117:416–427. <https://doi.org/10.1016/j.enconman.2018.09.088>
- Rabenstein G, Hacker V (2008) Hydrogen for fuel cells from ethanol by steam-reforming, partial oxidation and combined autothermal reforming : a thermodynamic analysis. *J Power Sources* 185:1293–1304. <https://doi.org/10.1016/j.jpowsour.2008.08.010>
- REN21 (2021) *Renewables 2021: Global Status Report*. [Accessed on 8<sup>th</sup> August 2021]
- Rodrigues A, Bordado JC, does Santos, R. G. (2017) Upgrading the glycerol from biodiesel production as a source of energy carriers and chemicals — a technological review for three chemical pathways. *Energies* 10(11):1817. <https://doi.org/10.3390/en10111817>
- Roslan NA, Asmawati A, Sumaiya Z, Ideris A, Vo DVN (2020) A review on glycerol reforming processes over Ni-based catalyst for hydrogen and syngas productions. *Int J Hydrogen Energy* 45(36):18466–18489. <https://doi.org/10.1016/j.ijhydene.2019.08.211>
- Said MSM, Ghani WAWAK, Tan HB, Ng DKS (2021) Prediction and optimisation of syngas production from air gasification of Napier grass via stoichiometric equilibrium model. *Energy Conversion Managt: X* 10:100057. <https://doi.org/10.1016/j.ecmx.2020.100057>
- Schwenber CA, Alves HJ, Schaffner RA, da Silva FA, Sequel R, Bach VR, Ferracin RJ (2016) Overview of glycerol reforming for hydrogen production. *Renew Sustain Energy Rev* 58:259–266. <https://doi.org/10.1016/j.rser.2015.12.279>
- Seadira T, Sadanandam G, Ntho TA, Lu X, Masuku CM, Scurrrell M (2018) Hydrogen production from glycerol reforming: conventional and green production. *Rev Chem Eng* 34(5):695–726. <https://doi.org/10.1515/revce-2016-0064>
- Tay DHS, Ng DKS, Kheireddine H, El-Halwagi MM (2011) Synthesis of an integrated biorefinery via the C-H-O ternary diagram. *Clean Tech Environ Policy* 13(4):567–579. <https://doi.org/10.1007/s10098-011-0354-4>
- Tay DHS, Kheireddine H, Ng DKS, El-Halwagi MM, Tan RR (2011) Conceptual synthesis of gasification-based biorefineries using thermodynamic equilibrium optimization models. *Ind Eng Chem Res* 50(18):10681–10695. <https://doi.org/10.1021/ie2009185>
- Tursi A (2019) A review on biomass : importance, chemistry, classification, and conversion. *Biofuel Res J* 22:962–979. <https://doi.org/10.18331/BRJ2019.6.2.3>
- Wang W (2010) Thermodynamic analysis of glycerol partial oxidation for hydrogen production. *Fuel Process Technol* 91(11):1401–1408. <https://doi.org/10.1016/j.fuproc.2010.05.013>
- WBA (2020) *Global Bioenergy Statistics 2020*. [Accessed on 8<sup>th</sup> August 2021]
- Yaws CL (1999) *Chemical properties handbook: physical, thermodynamic, environmental, transport, safety, and health related properties of organic and inorganic chemicals*. McGraw-Hill, Texas

- Zhang Z, Delcroix B, Rezazgui O, Mangin P (2020) Methanol production from pyrolysis oil gasification-model development and impacts of operating conditions. *Appl Sci* 10(20):7371. <https://doi.org/10.3390/app10207371>
- Zheng K, Lou HH, Gangadharan P, Kanchi K (2012) Incorporating sustainability into the conceptual design of chemical process-reaction routes selection. *Ind Eng Chem Res* 51(27):9300–9309. <https://doi.org/10.1021/ie3002952>

**Publisher's Note** Springer Nature remains neutral with regard to jurisdictional claims in published maps and institutional affiliations.

Springer Nature or its licensor holds exclusive rights to this article under a publishing agreement with the author(s) or other rightsholder(s); author self-archiving of the accepted manuscript version of this article is solely governed by the terms of such publishing agreement and applicable law.